

**Development of an OpenFOAM based Solver for Dilute
Laminar Gas-Droplet Flows with Evaporation and a
Proposal for a Turbulent Model**

A Thesis Submitted
in Partial Fulfilment of the Requirements
for the Degree of
Master of Technology

by
Nikhil R



भारतीय प्रौद्योगिकी संस्थान हैदराबाद
Indian Institute of Technology Hyderabad

**DEPARTMENT OF MECHANICAL & AEROSPACE
ENGINEERING
INDIAN INSTITUTE OF TECHNOLOGY
HYDERABAD**

JULY 2014

Declaration

I declare that this written submission represents my ideas in my own words, and where ideas or words of others have been included, I have adequately cited and referenced the original sources. I also declare that I have adhered to all principles of academic honesty and integrity and have not misrepresented or fabricated or falsified any idea/data/fact/source in my submission. I understand that any violation of the above will be a cause for disciplinary action by the Institute and can also evoke penal action from the sources that have thus not been properly cited, or from whom proper permission has not been taken when needed.



(Signature)

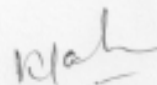
(Nikhil R)

ME12M1018

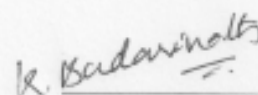
(Roll No.)

Approval Sheet

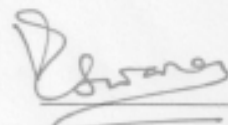
This Thesis entitled Development of an OpenFOAM based Solver for Dilute Laminar Gas-Droplet Flows with Evaporation and a Proposal for a Turbulent Model by Nikhil R is approved for the degree of Master of Technology from IIT Hyderabad



(Dr. Kirti Chandra Sahu) Examiner
Dept. of Chemical Eng
IITH



(Dr. Karri Badarinath) Examiner
Dept. of Mechanical and Aerospace Eng
IITH



(Prof. Vinayak Eswaran) Adviser
Dept. of Mechanical and Aerospace Eng
IITH

To my parents ...

Acknowledgements

I express my sincere gratitude to my thesis supervisor Prof. Vinayak Eswaran for his valuable guidance, timely suggestions and constant encouragement. His interest and confidence in me has helped immensely for the successful completion of this work. I am thankful to Narendra Gajbiye and Praveen Thovagunta for guiding me through the basics of Anupravaha and that way they gave a better knowledge about implementing a FVM based solver, which helped me in developing code in OpenFOAM. I would also like to thank Mrunalini, whose work has immensely helped me in my thesis.

I would like to specially thank my friends Ashwani Assam and Mohammadali Areekkadan who helped me in all difficult situations, I faced during my thesis work. I would like to thank all my faculties who helped me in building a strong base in the subjects, which helped me in my work. I would also like to thank all my classmates who made my stay in IIT Hyderabad memorable.

I would like to make a special mention of the excellent computational facilities provided by Prof. Vinayak Eswaran. I would like to thank the staff and fellow students in CAE and Heat Transfer Labs for creating a conducive environment to work in.

Finally, I would like to thank my parents for their constant support and encouragement and God for giving me a helping hand in difficult situations.

Nikhil R

Abstract

An OpenFOAM based solver for dilute laminar gas-droplet flows with evaporation is developed. The same module was implemented in a general purpose CFD solver, IITK-DAE ANUPRAVAHA SOLVER by Mrunalini [4] and Shashwat Swami Jaiswal [38]. A proposal for turbulent module for the same also has been made in this thesis.

The finite volume method with non-staggered grid arrangement has been used along with a fully implicit and semi-coupled algorithm to numerically solve the set of governing equations for laminar case. A two-way coupling has been assumed between the two phases. This has been achieved by including source terms in the governing equations, involving mass, momentum and energy transport between the phases. A classical model for droplet evaporation has been implemented in the OpenFOAM based solver. The solver has been successfully verified against the results of gas-droplet channel flow with evaporation against the results of Anupravaha and compared with that of the commercial software FLUENT.

A proposal for a two equation (k - ϵ) turbulent model for gas-droplet flows with evaporation has been made in this thesis. Taking the density variation in gaseous phase due to mixing into account, Favre-averaging is considered for this phase.

Contents

Declaration	ii
Approval Sheet	iii
Acknowledgements	iv
Abstract	v
List of Figures	x
1 Introduction	1
1.1 OpenFOAM	3
1.2 Gas Droplet Flows	3
1.3 Literature Review	4
1.4 Solution Methods	6
1.4.1 The Eulerian-Lagrangian Approach	6
1.4.2 The Eulerian-Eulerian Approach	7
1.5 The Two Fluid Model	8
1.6 Objectives of the Present Work	9
1.7 Thesis Organization	9
2 Governing Equations and Assumptions	10
2.1 Assumptions	10

2.2	The Governing Equations	11
2.2.1	The Gas-Phase	11
2.2.2	The Droplet Phase	12
2.3	Solution form of the governing equations	13
2.3.1	The Gas Phase	13
2.3.2	The Droplet Phase	14
2.4	The Boundary Conditions	15
2.4.1	At Solid Boundaries	15
2.4.2	Inlet	16
2.4.3	Outlet	16
2.5	Evaporation Model for Single Component Droplets	17
2.5.1	Classical D^2 -Law	17
2.5.2	Mathematical Formulations	19
2.5.3	Calculation of Rate of Evaporation	21
2.6	Unsteady-State Analysis	21
2.6.1	Calculation of heat flow rate and latent heat	21
2.7	Liquid Phase Analysis	22
2.8	Convective effects on evaporation	23
2.9	Property Evaluation	24
3	Discretization Procedure and Solution Algorithm	26
3.1	Description of the Finite Volume Method	26
3.2	Integral Form of Governing Equations	27
3.3	FVM for 3-D Geometry	28
3.4	Discretization Procedure	28
3.4.1	Discretization of the General Convection-Diffusion Equation	28
3.5	The Discretized Equations	30

3.5.1	The Gas Phase	30
3.5.2	The Droplet Phase	32
3.6	The Solution Algorithm	33
3.7	Summary of the Algorithm	38
3.8	Limiter for Θ_d equation	40
4	Results and Discussion	41
4.1	CASE 1: Gas-Droplet flow with $T_{di} = T_s$ and $u_{gi} = u_{di}$	42
4.2	CASE 2: Gas-Droplet flow with $T_{di} = T_s$ and $u_{gi} > u_{di}$	47
4.3	CASE 3: Gas-Droplet flow with $T_{di} = T_s$ and $u_{gi} < u_{di}$	50
4.4	CASE 4: Gas-Droplet flow with $T_{di} < T_s$ and $u_{gi} = u_{di}$	53
4.5	CASE 5: Gas-Droplet flow with isothermal walls	57
4.6	Closure	61
5	Proposal for Dilute Turbulent Gas-Droplet Flows with Evapora- tion Model	62
5.1	Properties of Turbulence	62
5.2	Reynolds Averaging	63
5.2.1	Eddy Viscosity Models	63
5.3	Favre Averaging	64
5.4	Assumptions	65
5.5	Favre averaged governing equations for the gas phase	65
5.5.1	Favre averaged continuity equation	66
5.5.2	Favre averaged momentum equation	66
5.5.3	Favre averaged temperature equation	68
5.5.4	Favre Averaged Species Mass Fraction Equation	70
5.6	Reynolds Averaged Equations for the Droplet Phase	70
5.6.1	Reynolds Averaged Continuity Equation	71

5.6.2	Reynolds Averaged momentum equation	71
5.6.3	Reynolds Averaged Temperature Equation	73
5.7	k - ϵ Equation of Gaseous Phase	73
5.8	Solution Algorithm	75
6	Conclusion and Scope of the Future work	77
A	Properties of fluids used	79
A.1	Properties of n-heptane	79
A.2	Properties of Air	80

List of Figures

2.1	Variation of temperature and gas concentration during droplet evaporation (Faeth) [13].	17
2.2	Burning rate curves for n-Heptane	18
4.1	The Computational Domain for 2D-Channel Flow Problems	41
4.2	Case 1: Contour plot for droplet volume fraction	43
4.3	Case 1: Contour plot for gas density (in kg/m^3)	44
4.4	Case 1: Contour plot for gas temperature (in K)	44
4.5	Case 1: Variation along the length of the channel	45
4.6	Case 1: Variation along the length of the channel	45
4.7	Case 1: Variation of Gas Temperature (in K) along the length of the channel	46
4.8	Case 2: Contour plot for droplet volume fraction	47
4.9	Case 2: Contour plot for evaporated fuel mass fraction	48
4.10	Case 2: Contour plot for gas density (in kg/m^3)	48
4.11	Case 2: Variation along the length of the channel	49
4.12	Case 2: Variation of Gas Temperature (in K) along the length of the channel	49
4.13	Case 3: Contour plot for droplet volume fraction	50
4.14	Case 3: Contour plot for evaporated fuel mass fraction	51
4.15	Case 3: Contour plot for gas density (in kg/m^3)	51

4.16 Case 3: Contour plot for gas temperature (in K)	52
4.17 Case 3: Variation along the length of the channel	52
4.18 Case 4: Contour plot for droplet volume fraction	53
4.19 Case 4: Contour plot for evaporated fuel mass fraction	54
4.20 Case 4: Contour plot for gas density (in kg/m^3)	54
4.21 Case 4: Contour plot for gas temperature (in K)	55
4.22 Case 4: Variation along the length of the channel	55
4.23 Case 4: Variation of Gas Temperature (in K) along the length of the channel	56
4.24 Case 5: Contour plot for droplet volume fraction	58
4.25 Case 5: Contour plot for evaporated fuel mass fraction	58
4.26 Case 5: Contour plot for gas density (in kg/m^3)	59
4.27 Case 5: Contour plot for gas temperature (in K)	59
4.28 Case 5: Variation along the length of the channel	60
4.29 Case 5: Variation of Gas Temperature (in K) along the length of the channel	60

Chapter 1

Introduction

Multiphase flow covers a vast field, a host of various technological events, a wide range of engineering disciplines, a number of natural processes. It encompasses a wide range of flow patterns and regimes. Virtually every processing technology must deal with multiphase flow, from electrographic processes to papermaking to cavitating pumps and turbines. Many diverse industries like aerospace, nuclear, water and transport, chemical, etc. encounter with multiphase flows. Many natural processes like formation and motion of rain drops, sand dunes formation are also coming under it. All these flows involve interaction between matter existing in different states. These interaction may be mass, momentum, energy or any of its combination. Multiphase flows can be quite complex and may involve various phases interacting simultaneously. It is useful to subdivide these vast field into a small number of identifiable classes.

The simplest of all multiphase flows are two-phase flows. Two-phase flow models can be explored either experimentally or numerically. But experimental modelling can be quite expensive and difficult to set-up. Moreover in many instances, it requires to have a different scale than the prototype and then a proper numerical model is required for confident extrapolation to the scale of prototype. In this work, mathematical modeling of two-phase flows involving gas and evaporating liquid droplets is attempted considering certain assumptions. The development of accurate mathematical models of two-phase flows is important for optimum design and control of various industrial systems. Mathematical modeling of two-phase flows poses several challenges as the problem involves rapidly changing and/or moving interfaces and continuous interaction between the phases which affect the behavior of each of the interacting phases. In this work, we

numerically solve dilute dispersed two-phase flows using the three fundamental principles that govern any fluid flow: (i) mass conservation, (ii) momentum conservation and (iii) energy conservation. A brief introduction to two-phase flows is given below.

Two phase flows, in general, can be characterized both by the combination of interacting phases and also by the interface structures. Classification based on the state of the constituents of the flow is as follows:

1. Gas-liquid (bubbly flows, slug flows, gas-droplet)
2. Liquid-solid (slurry flows, sediment transport)
3. Gas solid (particle laden flows, fluidized beds)
4. Liquid-liquid(flow of immiscible liquids)

On the basis of configuration two-phase flows are classified as follows:

1. Dispersed flows, in which the two phases are thoroughly mixed in each other.
2. Free surface flows (separated flows), in which the two phases are separated by a distinct interface.

Dispersed flows consist of finite particles, droplets, bubbles distributed in a connected volume of continuous phase. It is further divided into three regimes by considering the phase of dispersion as follows:

1. Bubbly flows
2. Droplet flows
3. Particle flows

This thesis involves numerical modeling of dilute dispersed gas-droplet flows involving gas and evaporating liquid droplets. Droplets are called as the disperse phase and the fluid in which the droplets move is called as continuous phase.

In this work, dilute droplet flows with evaporation in a gas phase is being mathematically modelled as a part of OpenFOAM(Open Field Operation And

Manipulation) solver. It is a free, open source CFD software package developed by OpenCFD Ltd at ESI Group and distributed by the OpenFOAM Foundation. Usage of an open source software package is cost-effective compared to some commercial packages as those charge money for their use. Tracking of interface between the various phases is a major component of separated flow algorithms, which usually is not attempted for disperse phase flows. For dispersed flows, the mixture is characterized by volume-fraction, without making reference to the shape of the actual interfaces between the phases. This procedure is described elaborately in Section 1.4.3. A brief introduction about OpenFOAM is given in the following Section 1.1 .

1.1 OpenFOAM

OpenFOAM is first and foremost a C++ library, used primarily to create executables, known as applications. The applications fall into two categories: solvers, that are each designed to solve a specific problem in continuum mechanics; and utilities, that are designed to perform tasks that involve data manipulation and algebraic calculations. OpenFOAM is distributed with a large set of precompiled applications but users also have the freedom to create their own or modify existing ones. It is divided into a set of precompiled libraries that are dynamically linked during compilation of the solvers and utilities. Libraries such as those for physical models are supplied as source code so that users may conveniently add their own models to the libraries. Meshes can be generated in two ways in OpenFOAM. Either it uses the blockMesh utility for generating simple meshes of blocks of hexahedral cells or convertMesh utility to convert meshes generated by some third party software into the format that it can read.

Post-processing in OpenFOAM can either be done using paraFoam utility, which uses paraView, an open source visualisation application or using some other third party post processing softwares like EnSight, Fieldview etc..

1.2 Gas Droplet Flows

Dispersed gas-liquid flows are encountered in many engineering applications. Evaporating sprays are used in gas turbine systems, internal combustion engines

and fire safety systems (Faeth [13]). Laminar and turbulent gas droplet flows are used in emergency core cooling systems of nuclear reactors (Hwang [43]). Gas droplet flows may be dilute as well as dense. In dense gas droplet flows the interaction between the droplets is of prime importance. That means a three-way coupling is to be considered. On the other hand a dilute gas-droplet flow does not require the consideration of droplet-droplet interactions and the effect of adjacent drops on drop transport rates. In this case depending on the droplet concentration a one-way or a two-way coupling between the phases will suffice.

A one-way coupling indicates that the droplets are affected by the fluid flow, but not vice-versa; in two-way coupling the two phases influence each other. It follows therefore that for very low particle concentrations a one-way coupling is sometimes enough to model the interactions whereas for somewhat denser flows a two-way coupling must be considered. In this work, to take into account the mass, momentum and energy transfer between the droplet and the surrounding gas, two-way coupling is employed. Interaction between droplets i.e. droplet collisions and break-ups are not considered in this study.

1.3 Literature Review

Research in the field of two-phase flows has been carried out for decades. The fundamental concept of the two-fluid model is first discussed in detail in the book by Ishii [1]. The classification of the multiphase flow is also discussed in his book. The governing equations used for both the phases in two-continua formulation is given in the book by Sirignano [2]. Previous research on two-fluid modeling is reported by Crowe et al. [3], Darwish [5], Hallmann [6] and Guo et al. [7]. The parameters used in the study as volume fraction, number density are described in detail with various averaging procedures in Crowe et al. [3].

The simplest model for droplet evaporation was first suggested by Maxwell back in 1877 [8]. According to this model, the rate of evaporation is controlled exclusively by the diffusion process. His model ignores the effect of the convective flow of the mixture of gas and fuel vapour away from the surface of the droplet. The classical d^2 -law of evaporation is formulated by Godsave [9] and Spalding [10] for single isolated droplet evaporating in a quiescent environment. To take into account the effect of the convective flow of the surrounding gas, which en-

hances the heat and mass transfer between the droplet and the gas phase, many researchers have given correction factors for the basic models. In a comprehensive theoretical and experimental study, Frossling [11] first showed that effects of convection on heat and mass transfer rates could be accommodated by a correction factor that is a function of Reynolds number and Schmidt's (or Prandtl) number. The original correlation has been later modified by Ranz and Marshall [12]. Later Faeth [13] analyzed the available data on convective effects and proposed a synthesized correlation. The present study uses the correlation given by Ranz and Marshall [12]. In this study separate evaporation model for laminar and turbulent flows are proposed.

The evaporation model for laminar flow used in the present study is essentially the classical model of Spalding [10]. The model used is described in the book on 'Atomization and Sprays' by Lefebvre [14]. Kent [15] studied the diffusion controlled droplet evaporation and condensation and discussed the effect of free-stream fuel vapour mass fraction on drop evaporation. Sazhin [16] reviewed the recent developments in modeling the heating and evaporation of fuel droplets. In the present study 'rapid mixing model' for the liquid droplet described in Faeth [13] and Chen [37] is used. This simplifies the analysis by assuming infinite conductivity of the liquid. However, it may lead to small error in the solution. For the liquid droplet phase analysis Abramzon et al.[17] used effective conductivity model. Expressions for the variation of properties of gases and liquids used in this study are taken from Perry [18] and Reid [19]. Hubbard et al. [20] studied the effect of transient and variable properties on drop evaporation rate, and showed that the '1/3' rule worked well as a mixing rule. In the present evaporation model for laminar flow this rule is used for the calculation of the properties at droplet surface based on average temperature and composition.

Physics of Turbulent flow is explained in detail in Pope[22] and Wilcox[23]. Taking into consideration of the density variation effect, mass-averaging of turbulent quantities are required. It is explained in Todd[24]. Various existing analytical descriptions for predicting turbulent flows-laden with solid particles/liquid droplets are reviewed in Mashayek[25]. Study of two-dimensional turbulent gas flows with particle deposition by Eulerian-Two Fluid approach is explained in Slater[26]. Complex turbulent interactions between phases are explained in Patrick[27]. Effect of turbulence on mass transfer from a single fuel droplet is dealt with in

Al-Sood[28].

In the literature, there are many experimental studies dealing with droplet evaporation. However, there are only few studies that come to the basic and ideal case of a single droplet evaporation in a quiescent or convective environment. A large number of studies consider multi-component droplets in turbulent evaporating sprays, jets with different classes of droplets where each class refers to a group of droplets of same diameters having their own volume fraction, mass flow rates. Some of droplet flow experimental results are given in Downing [29], Ranz and Marshall [12], Chin and Lefebvre [30], Kolaitis [31] and Miller et al. [32]. For the study of laminar gas-droplet flows in one of the cases we have assumed the initial droplet temperature is the saturation temperature, to simplify the analysis as discussed in Mongia et al.[33] and Elghobashi et al.[34].

1.4 Solution Methods

Models for two-phase flows can be categorized into two different groups. In the first group, there are models that track the interface between the two phases. These are ideal models for separated flows. In the second group, there are models where the exact position of the interface is not followed specifically. Dispersed flows are usually modeled using models from this second group. The complexity of the interfaces between the two phases in dispersed flow is too high for interface tracking methods to be suitable, at least with today's computing capacity. To model this type of flows, another strategy is needed. There are two generic approaches for modeling gas-disperse phase flows: Eulerian-Eulerian approach and the Eulerian-Lagrangian approach.

1.4.1 The Eulerian-Lagrangian Approach

In this approach, the general idea is to follow each particle or droplet of the flow as they advect in the continuous phase. This approach is referred to as the Eulerian-Lagrangian method, where the continuous phase is treated as a continuum and calculated in an Eulerian reference frame, while particles (or interfaces) of the disperse phase are tracked using a Lagrangian approach. In this approach the inter-phase transfer terms are calculated for the disperse phase while tracking the droplets or particles and then they are used in the Eulerian form of the

equations of the continuous phase. The Eulerian-Lagrangian approach works well for few particles/interfaces. However, for a large number of particles the Eulerian-Lagrangian approach becomes computationally expensive.

1.4.2 The Eulerian-Eulerian Approach

A different way of modeling dispersed flows is to treat both the phases as a continuum. This is generally referred to as Eulerian-Eulerian approach or two-fluid model, first discussed by Ishii [1]. In this case local instantaneous equation of mass, momentum and energy balance for both phases are derived along with source terms for interaction between the phases. A very important concept in the Eulerian-Eulerian approach is that of the volume fraction or volume concentration which is defined in the section 1.5.

Depending on the way the phases interact the following modeling approaches are used within the perview of the Eulerian-Eulerian method:

1. The Homogeneous Equilibrium Model
2. The Drift Flux Model
3. Two Fluid Model

In the homogeneous equilibrium model the flow is analyzed by treating the flow as a mixture, whose properties are determined based on the properties of its constituents as well as the proportion of the constituents in the mixture.

Drift flux model is similar to the homogeneous equilibrium model but it takes into account for the slip between the phases, and so additional terms appear in the equations. The drift flux model and the homogeneous models are sometimes referred to as mixture models.

In the two fluid model both the phases have their own velocity and temperature field and other properties. The interaction between the two phases is taken care of by including exchange coefficients. This is the method adopted in this work¹. The details of the same can be found in section 1.5. One drawback of this approach is implementation of exchange coefficients.

¹Although, it must be noted that the detailed flow field *within* droplets are not obtained. Rather, the average momentum of droplets are computed.

1.5 The Two Fluid Model

In the present work an Eulerian-Eulerian two fluid model is used to simulate the flows. Both the phases are treated as inter-penetrating continua and mass, momentum and energy equations are solved to obtain the velocity and temperature fields for the phases. The volume fraction is also solved for by solving a convection equation. Details of the governing equations are given in Chapter 2. Each dependent variable at any special point is an instantaneous average value over a neighbourhood of that point that includes both liquids and gas. Therefore both liquid properties and gas properties exist at a point, regardless of whether that point is actually in a gas or in a liquid at that instant. This method is a two-continua approach since both a continuum of gas properties and a continuum of liquid properties are defined.

Now we define some properties of the droplet-phase flows. The volume fraction of a phase is defined as the ratio of the volume occupied by that phase to the total volume under consideration. Mathematically we can write

$$\vartheta_d = \lim_{\Delta V \rightarrow 0} \frac{\Delta V_d}{\Delta V}$$

Here ϑ_d denotes the volume fraction of the disperse phase, and ΔV_d is the volume occupied by that phase in the neighbourhood of the point of interest, whereas ΔV is the total volume occupied by the two phases in the neighborhood of the point. Defined in this way, ϑ becomes a function with a value at each point. In the Eulerian-Eulerian framework ϑ is assumed to be a continuous variable and often transport equations are solved for it. Equivalently, the volume fraction of the continuous phase or void fraction is given as

$$\vartheta_g = \lim_{\Delta V \rightarrow 0} \frac{\Delta V_g}{\Delta V}$$

Here ϑ_g denotes the volume fraction of the continuous phase, and ΔV_g is the volume occupied by the continuous phase in the neighbourhood of the point of interest. So the summation of the volume fractions must be unity, $\vartheta_g + \vartheta_d = 1$. Note that for *dilute* two-phase flows $\vartheta_g \approx 1$. Another important parameter, number density is defined as the number of particles or droplets per unit volume, we can write it as

$$n = \lim_{\Delta V \rightarrow 0} \frac{\Delta N}{\Delta V}$$

also,

$$n = \frac{6\vartheta_d}{\pi d_d^3} \quad (1.1)$$

where n denotes the number density of the disperse phase, and ΔN is the number of elements in the volume and d_d is diameter of the droplets (which are assumed to be of the same size).

1.6 Objectives of the Present Work

1. To develop a module in OpenFOAM to solve dilute laminar gas-droplet flows with evaporation using an Eulerian-Eulerian framework.
2. To validate the solver by comparing the results with those obtained using another solver IITK-DAE Anupravaha, which was validated against commercial package Fluent.
3. To propose a model for dilute turbulent gas-droplet flows with evaporation along with the solution algorithm.

1.7 Thesis Organization

The thesis is organized in the following way. Chapter 2 deals with the assumptions, governing equations and boundary conditions. Chapter 3 includes the discretization procedure and the solution algorithm. Chapter 4 deals with the results obtained using the OpenFOAM solver, and comparisons with IITK-DAE Anupravaha and Fluent, Chapter 5 presents the proposal for dilute turbulent gas-droplet flows with evaporation, which is followed by discussions.

Chapter 2

Governing Equations and Assumptions

An Eulerian two-fluid model is employed in the present study. It considers the gas and the droplet phases as two interpenetrating continua. This chapter presents the laminar flow model that was developed by Mrunalini in [4] and other previous M.Tech students of Prof.Vinayak Eswaran. The derivations of the equations prescribed in this chapter are given in Mrunalini [4]. A two-way coupling between the two phases is achieved by including the mass, momentum and energy transfer terms between the phases in the governing equations for both the phases. It is derived based on the following assumptions:

2.1 Assumptions

1. The spray is assumed to be *dilute* ($\vartheta_d < 0.1\%$) . Under this assumption droplet collisions are ignored and the effect of adjacent drops on drop transport rates are neglected. Also viscous stresses, and temperature and pressure variation *within* the dispersed phase are neglected.
2. At each location of the flow field, droplet-phase and gas -phase co-exist and inter-penetrate with each other, each having its own velocity and temperature.
3. The flow around the droplet is assumed to be quasisteady, that means the flow immediately adjusts to the local boundary conditions. This allows the use of drag coefficient formulations to represent the interphase forces on the droplets.

4. The droplets are assumed to be spherical and mono-sized.
5. The radial velocity of the liquid surface due to the evaporation of the liquid is neglected.
6. Effects of drag and forced convection are represented by empirical relations.
7. It is assumed that the only significant interphase force is due to drag. This is true for large droplet-to-gas density ratios $(\rho_d/\rho_g) > 600$.
8. During the evaporation process, droplets do not break-up and chemical reaction is also neglected.
9. The gas phase Lewis number is assumed to be unity.

2.2 The Governing Equations

2.2.1 The Gas-Phase

The governing equations for the gas phase are the Navier Stokes equations, energy equation and mass fraction equation with extra source terms that reflects the contribution of the droplet phase on the gas phase. In Cartesian coordinates the equations are as below.

Continuity:

$$\frac{\partial \vartheta_g \rho_g}{\partial t} + \nabla \cdot (\vartheta_g \rho_g \mathbf{u}_g) = n \dot{m}_v \quad (2.1)$$

Momentum:

$$\frac{\partial (\vartheta_g \rho_g \mathbf{u}_g)}{\partial t} + \nabla \cdot (\vartheta_g \rho_g \mathbf{u}_g \mathbf{u}_g) = \nabla \cdot (\mu_g \vartheta_g \nabla \mathbf{u}_g) - \vartheta_g \nabla P + \vartheta_g \rho_g \mathbf{g} + n \dot{m}_v \mathbf{u}_d - \vartheta_d \mathbf{f}_d \quad (2.2)$$

Energy:

$$\frac{\partial (\vartheta_g \rho_g C_{pg} T_g)}{\partial t} + \nabla \cdot (\vartheta_g \rho_g C_{pg} T_g \mathbf{u}_g) = \nabla \cdot (\vartheta_g k_g \nabla T_g) + n \dot{m}_v C_{vd} T_d - n Q \quad (2.3)$$

Species Mass Fraction: As evaporation from the droplets is also considered, it is assumed that the evaporated vapour is of a different species (say, fuel) than the ambient gas. Therefore, an equation for the species Y_F is also solved:

$$\frac{\partial (\vartheta_g \rho_g Y_F)}{\partial t} + \nabla \cdot (\vartheta_g \rho_g Y_F \mathbf{u}_g) = \nabla \cdot (\vartheta_g \rho_g D \nabla Y_F) + n \dot{m}_v \quad (2.4)$$

where ϑ_g is gaseous phase volume fraction, ρ_g is the density of the gas phase, \mathbf{u}_g and T_g are velocities and temperature of the gas phase respectively. Y_F is the evaporated fuel mass fraction, μ is viscosity, C_{pg} is the specific heat at constant pressure, k_g is thermal conductivity of the gas phase, \mathbf{g} is acceleration due to gravity. \dot{m}_v is the evaporation rate for a single droplet, n is the number density, C_{vd} is the specific heat of the *vapour* phase of the liquid in the droplet, T_d is droplet temperature, D is the diffusion coefficient of fuel vapour in gas and Q is heat transfer from the gas to a single drop, \mathbf{f}_d the drag force acting on the droplet per unit volume. This is described in next section, 2.2.2.

2.2.2 The Droplet Phase

The governing equations for the droplet phase are:

Continuity:

$$\frac{\partial (\rho_d \vartheta_d)}{\partial t} + \nabla \cdot (\rho_d \vartheta_d \mathbf{u}_d) = -n \dot{m}_v \quad (2.5)$$

Momentum:

$$\frac{\partial \rho_d \vartheta_d \mathbf{u}_d}{\partial t} + \nabla \cdot (\rho_d \vartheta_d \mathbf{u}_d \mathbf{u}_d) = -\vartheta_d \nabla P + \vartheta_d \rho_d \mathbf{g} - n \dot{m}_v \mathbf{u}_d + \vartheta_d \mathbf{f}_d \quad (2.6)$$

where ϑ_d is the volume fraction, ρ_d is the material density of the droplet phase and \mathbf{u}_d is local velocity of the droplets. The term $(\vartheta_d \mathbf{f}_d)$ in equations 2.2 and 2.6 is the drag force acting on the droplet phase per unit volume and is given by (Kolev [45]):

$$\mathbf{f}_d = \rho_g \frac{1}{\left(\frac{4}{3} \pi \left\{\frac{d_d}{2}\right\}^3\right)} \frac{1}{2} C_d |\mathbf{u}_g - \mathbf{u}_d| (\mathbf{u}_g - \mathbf{u}_d) \left(\frac{\pi}{4} d_d^2\right) = \beta (\mathbf{u}_g - \mathbf{u}_d)$$

where, d_d is the diameter of the droplets and C_d is the drag coefficient which is given by (Kolev [45]):

$$C_d = \begin{cases} \frac{24}{Re_d} & \text{if } Re_d \leq 1 \\ \frac{24}{Re_d} (1 + 0.15 Re_d^{0.687}) & \text{if } 1 \leq Re_d \leq 1000 \\ 0.44 & \text{otherwise} \end{cases}$$

Here Re_d is the *droplet Reynolds number*, defined as (Miller et al. [32])

$$Re_d = \frac{\rho_g |\mathbf{u}_g - \mathbf{u}_d| d_d}{\mu_g}$$

Energy:

$$\frac{\partial [\rho_d \vartheta_d C_{ld} T_d]}{\partial t} + \nabla \cdot (\rho_d \vartheta_d C_{ld} T_d \mathbf{u}_d) = -n \dot{m}_v C_{ld} T_d - n \dot{m}_v L + n Q \quad (2.7)$$

where T_d is droplet temperature and L is the latent heat of vaporization of the liquid droplet at the droplet temperature.

2.3 Solution form of the governing equations

2.3.1 The Gas Phase

The continuity equation for the gas phase (equation 2.1) may be written as:

Since $\vartheta_g = 1 - \vartheta_d \simeq 1$, we take it out of the derivatives.

$$\frac{\partial \rho_g}{\partial t} + \nabla \cdot (\rho_g \mathbf{u}_g) = \frac{1}{\vartheta_g} n \dot{m}_v \quad (2.8)$$

or

$$\frac{\partial \rho_g}{\partial t} + \mathbf{u}_g \cdot \nabla \rho_g + \rho_g \nabla \cdot \mathbf{u}_g = \frac{1}{\vartheta_g} n \dot{m}_v \quad (2.9)$$

or,

$$\frac{D \rho_g}{Dt} + \rho_g \nabla \cdot \mathbf{u}_g = \frac{1}{\vartheta_g} n \dot{m}_v \quad (2.10)$$

The right side terms of the above equations signifies the mass transfer between the phases due to the evaporation of droplets. This emphasizes the fact that we must enforce continuity at each timestep by solving this equation for density.

Using the above equations, the momentum, energy and species mass fraction equations for the gas phase (equation 2.2 , 2.3 and 2.4) can be re-written as,

Momentum:

$$\begin{aligned} \frac{\partial \mathbf{u}_g}{\partial t} + \nabla \cdot (\mathbf{u}_g \mathbf{u}_g) = & \frac{1}{\rho_g} [\nabla \cdot (\mu_g \nabla \mathbf{u}_g)] - \frac{1}{\rho_g} \nabla P + \mathbf{g} - \frac{1}{\vartheta_g \rho_g} [n \dot{m}_v \mathbf{u}_g] \\ & + \frac{1}{\vartheta_g \rho_g} [n \dot{m}_v \mathbf{u}_d] - \frac{\vartheta_d}{\vartheta_g \rho_g} \mathbf{f}_d \quad (2.11) \\ & + \mathbf{u}_g [\nabla \cdot \mathbf{u}_g] \end{aligned}$$

Energy:

$$\frac{\partial (C_{pg} T_g)}{\partial t} + \nabla \cdot (C_{pg} T_g \mathbf{u}_g) = \frac{1}{\rho_g} [\nabla \cdot (k_g \nabla T_g)] + \frac{1}{\vartheta_g \rho_g} [n \dot{m}_v C_{vd} (T_d - T_g)] - \frac{n Q}{\vartheta_g \rho_g} + C_{pg} T_g [\nabla \cdot \mathbf{u}_g] \quad (2.12)$$

where, it may be noted, the gas density ρ_g has been taken out of the partial differentials.

Species Mass Fraction:

$$\frac{\partial Y_F}{\partial t} + \nabla \cdot (Y_F \mathbf{u}_g) = \frac{1}{\rho_g} [\nabla \cdot (\rho_g D \nabla Y_F)] + \frac{n \dot{m}_v}{\vartheta_g \rho_g} (1 - Y_F) + Y_F [\nabla \cdot \mathbf{u}_g] \quad (2.13)$$

In the above equations gas phase specific heat C_{pg} and thermal conductivity k_g are computed by mixing laws as a mass fraction average of pure species specific heat and thermal conductivity as follows,

$$C_{pg} = Y_F C_{vd} + (1 - Y_F) C_{pc} \quad \text{and} \quad k_g = Y_F k_{vd} + (1 - Y_F) k_c \quad (2.14)$$

where C_{pc} and k_c are the specific heat and thermal conductivity for pure gas respectively, while subscript 'vd' stands for the vapour evaporated from the droplets.

2.3.2 The Droplet Phase

The continuity equation for the droplet phase is written as,

$$\frac{\partial (\rho_d \vartheta_d)}{\partial t} + \nabla \cdot (\rho_d \vartheta_d \mathbf{u}_d) = -n \dot{m}_v \quad (2.15)$$

or

$$\frac{\partial (\rho_d \vartheta_d)}{\partial t} + \mathbf{u}_d \cdot \nabla (\rho_d \vartheta_d) + (\rho_d \vartheta_d) \nabla \cdot \mathbf{u}_d = -n \dot{m}_v \quad (2.16)$$

or,

$$\frac{D (\rho_d \vartheta_d)}{Dt} + (\rho_d \vartheta_d) \nabla \cdot \mathbf{u}_d = -n \dot{m}_v \quad (2.17)$$

$$\frac{D\vartheta_d}{Dt} + \vartheta_d \nabla \cdot \mathbf{u}_d = -\frac{n\dot{m}_v}{\rho_d} \quad (2.18)$$

For dilute two-phase flows, $\vartheta_d < 0.1\%$. Hence, for computational ease, we normalize the volume fraction equation by considering the initial volume fraction as ϑ_0 and define the normalized volume fraction of the dispersed phase as Θ_d .

$$\Theta_d = \frac{\vartheta_d}{\vartheta_0} \quad (2.19)$$

$$\frac{D\Theta_d\vartheta_0}{Dt} + \Theta_d\vartheta_0 \nabla \cdot \mathbf{u}_d = -\frac{n\dot{m}_v}{\rho_d} \quad (2.20)$$

Taking ϑ_0 to RHS, we get

$$\frac{D\Theta_d}{Dt} + \Theta_d \nabla \cdot \mathbf{u}_d = -\frac{n\dot{m}_v}{\rho_d\vartheta_0} \quad (2.21)$$

Momentum: The momentum equation can be simplified as,

$$\frac{\partial \mathbf{u}_d}{\partial t} + \nabla \cdot (\mathbf{u}_d \mathbf{u}_d) = -\frac{1}{\rho_d} \nabla P + \mathbf{g} + \frac{1}{\rho_d} \mathbf{f}_d + \mathbf{u}_d [\nabla \cdot \mathbf{u}_d] \quad (2.22)$$

Energy:

$$\frac{\partial C_{ld} T_d}{\partial t} + \nabla \cdot (C_{ld} T_d \mathbf{u}_d) = -\frac{n\dot{m}_v L}{\rho_d \vartheta_d} + \frac{nQ}{\rho_d \vartheta_d} + C_{ld} T_d [\nabla \cdot \mathbf{u}_d] \quad (2.23)$$

2.4 The Boundary Conditions

2.4.1 At Solid Boundaries

At solid boundaries a no-slip condition is specified for the gas phase. Hence at the solid boundaries,

$$u_g = 0, \quad v_g = 0, \quad w_g = 0.$$

For the pressure it is usual to specify a homogeneous Neumann boundary condition, that is

$$\frac{\partial P}{\partial n} = 0$$

where n is the coordinate normal to the wall.

For the droplet phase a free-slip boundary condition is assumed at the wall. Hence we have

$$\begin{aligned} u_{d,n} &= 0 \\ \frac{\partial u_{d,t}}{\partial n} &= 0 \end{aligned}$$

where n , t is the wall normal and tangential component of velocity, respectively. For volume fraction, fuel mass fraction and droplet temperature a homogeneous Neumann boundary condition is specified at the walls.

$$\frac{\partial \phi}{\partial n} = 0$$

where ϕ is ϑ_d , Y_F and T_d .

2.4.2 Inlet

At the inlet, all variables other than pressure are specified.

$$\phi = \phi_{in}$$

where ϕ is any variable except pressure. The boundary condition for pressure is once again assumed to be of homogeneous Neumann type,

$$\frac{\partial P}{\partial n} = 0$$

2.4.3 Outlet

At the outlet a homogeneous Neumann condition is assumed for all flow variables except pressure.

$$\frac{\partial \phi}{\partial n} = 0$$

where ϕ is any variable except pressure. For pressure any value may be specified, because it is only the pressure gradient that is important, and not the absolute pressure. It is convenient to specify a homogeneous Dirichlet condition for pressure at the outlet.

$$P = 0$$

2.5 Evaporation Model for Single Component Droplets

2.5.1 Classical D^2 -Law

The classical D^2 -law was formulated in the 1950s by Godsave [9] and Spalding [10]. It was derived for an isolated, pure-component droplet burning in a quiescent, oxidizing environment. It has since then been termed the D^2 -law, because it predicts that the square of the droplet diameter decreases linearly with time. The model can be used both for the combustion and for the evaporation of a droplet.

A sketch of the droplet evaporation process is provided in Fig. 2.1, for the hypothetical case where a pure fuel drop is suddenly introduced into a gas at elevated temperature. At typical injection temperatures, the fuel concentration at liquid surface is low, and there is little mass diffusion from the drop early in the process. Under these conditions, the droplet heats up, much like a cold body placed in a heated environment. In general, temperatures are not uniform within the droplet but is lower at the center of the drop, with the maximum liquid temperature at the surface.

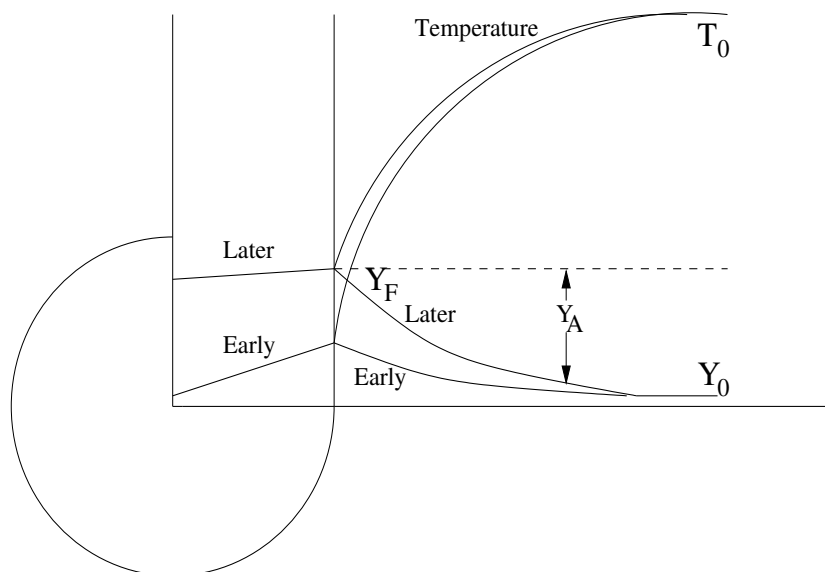


Figure 2.1: Variation of temperature and gas concentration during droplet evaporation (Faeth) [13].

Initially, almost all of the heat supplied to the drop serves to raise its tem-

perature. As the liquid temperature rises, the fuel vapour formed at the liquid surface has two effects i.e., an increasing portion of the energy reaching the drop surface must supply the heat of vaporization of the evaporating fuel, and the outward flow of the fuel vapour reduces the heat transfer to the droplet. This slows the rate of increase of the liquid surface temperature and therefore, later in the process, the temperature becomes relatively uniform in the droplet. Eventually, a stage is reached where all the heat reaching the surface is utilized for the heat of vaporization and the droplet stabilizes at a temperature called the “wet bulb temperature”. The droplet attains its steady-state and the drop diameter diminishes with time according to the relationship ([10],[9])

$$d_0^2 - d^2 = \lambda_{st}t \quad (2.24)$$

Burning rate curves are shown in Fig. 2.2 for n-Heptane which for the studied case has $\lambda_{st} = 0.30 \text{ mm}^2/\text{s}$.

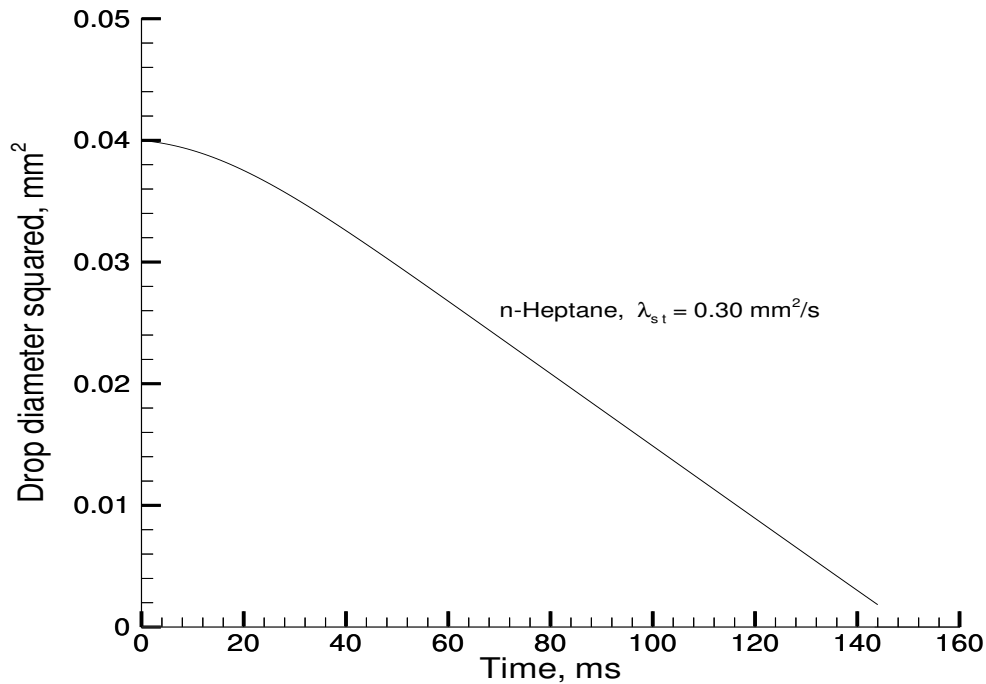


Figure 2.2: Burning rate curves for n-Heptane

2.5.2 Mathematical Formulations

Evaporation process involves both heat and mass transfer. Rate of mass transfer from droplets to gas and rate of heat transfer from gas to droplets are required to analyse the evaporation rate of the droplets. Two parameters, mass transfer number (B_M) and heat transfer number (B_T) are used to measure mass and heat transfer rates.

Mass transfer number

An expression for the rate of evaporation of a fuel drop is derived as follows. Neglecting thermal diffusion and assuming that the driving force for species diffusion is a concentration gradient in the direction of the diffusion path, the following expression is obtained for an evaporating drop [14]:

$$\frac{dY_F}{dr} = -\frac{RT}{D_c P} (m_F Y_A) \quad (2.25)$$

Y_F = fuel mass fraction

Y_A = air mass fraction

m_F = mass rate of diffusion per unit area

D_c = diffusion coefficient

P = gas pressure

r = radius ($r = 0$ at center of drop and $r = r_s$ at drop surface)

The boundary conditions are

$$\begin{array}{lll} r = r_s; & T = T_s; & Y_F = Y_{Fs} \\ r = \infty; & T = T_\infty; & Y_F = Y_{F\infty} = 0 \end{array}$$

Integrating Eqn. 2.25 between $r = r_s$ and $r = \infty$ gives

$$\dot{m}_v = 2\pi d_d \rho D_c \ln(1 - Y_{Fs}) \quad (2.26)$$

Assuming the Lewis number ($Le \equiv \frac{\alpha}{D}$) is equal to unity, the quantity ρD_c can be replaced by (k_{gref}/C_{pgref}) , where k_{gref} and C_{pgref} are the mean thermal conductivity and specific heat, respectively.

Defining

$$B_M = \frac{Y_{F_s} - Y_{F_\infty}}{(1 - Y_{F_s})} \quad (2.27)$$

Now substituting B_M in Eq. 2.26 gives [14]

$$\dot{m}_v = 2\pi d_d \left(\frac{k}{C_p} \right)_{g_{ref}} \ln(1 + B_M) \quad (2.28)$$

This is the basic equation for the evaporation rate of a fuel drop of diameter d_d . Its accuracy is very much dependent on the choice of the values of $k_{g_{ref}}$ and $C_{pg_{ref}}$. The reference temperature and composition for the evaluation of the average properties will be discussed later in this chapter.

Heat transfer number

Similar to the above analysis but based on the convective and conductive heat fluxes across a thin shell surrounding the evaporating drop, lead to the following expression for heat transfer number [10]:

$$B_T = \frac{C_{pg_{ref}}(T_\infty - T_s)}{L} \quad (2.29)$$

where L is the latent heat of vaporization of fuel at droplet surface temperature T_s .

The number B_T denotes the ratio of the available enthalpy in the surrounding gas to the heat required to evaporate the fuel. In this case the rate of evaporation for Lewis number of unity is obtained as

$$\dot{m}_v = 2\pi d_d \left(\frac{k}{C_p} \right)_{g_{ref}} \ln(1 + B_T) \quad (2.30)$$

Under the steady-state condition $B_M = B_T$ and either Eq. 2.28 or Eq. 2.30 may be used to calculate the rate of evaporation. The advantage of Eq. 2.28 is that it applies under all conditions, including the transient state of droplet heat-up, whereas Eq. 2.30 can only be used for steady-state evaporation. However, Eq.2.30 is usually easier to evaluate, since the magnitudes of various terms are either contained in the data of the problem or readily available in the literature. This is particularly true when the ambient gas temperature is significantly higher than the fuel surface temperature T_s , then T_s can be replaced by the boiling temperature of the fuel with little loss in accuracy.

2.5.3 Calculation of Rate of Evaporation

The fuel vapour mass fraction at the droplet surface is calculated by taking the partial pressure weighted average of molecular weights,

$$Y_{F_S} = \left[1 + \left(\frac{P}{P_{F_S}} - 1 \right) \frac{M_A}{M_F} \right]^{-1} \quad (2.31)$$

In any given calculation, P , M_A , M_F , and T_∞ are known. All other terms are functions of T_S . A modified form of Clausius-Clapeyron equation for saturation pressure [14] gives us

$$P_{F_S} = \exp \left(a - \frac{b}{T_s - 43} \right) \text{ kPa} \quad (2.32)$$

Eqns. 2.31 and 2.32 form a set of equations for the two unknowns Y_{F_S} and T_S . Having obtained these values, mass evaporation rate for the drop can be calculated from equation 2.28 or 2.30.

2.6 Unsteady-State Analysis

Fig. 2.2 shows a straight line relationship between droplet diameter squared and time during most of the evaporation period. However, inspection reveals that in the first stage of evaporation, slope of d_d^2/t line is not constant; actually at the start it is almost zero and then it gradually increases with time until the droplet attains its wet-bulb temperature, after which slope remains constant throughout its lifetime.

For the purpose of analysis the vaporization process is divided into the transient or unsteady state and the steady state. The magnitude of the unsteady portion depends on many parameters such as properties of fuel, ambient pressure and temperature and initial temperature of the drop.

2.6.1 Calculation of heat flow rate and latent heat

A quasi-steady gas phase is assumed in which the boundary layer around the drop has the same characteristics as a steady boundary layer for the same conditions of drop size, velocity, surface temperature and ambient temperature. The heat transfer coefficient is given by [14]

$$Nu = \frac{h d_d}{k_{g_{ref}}} = 2 \frac{\ln(1 + B_M)}{B_M} \quad (2.33)$$

The heat transferred from the gas to the drop is

$$Q = \pi d_d^2 h (T_\infty - T_s) \quad (2.34)$$

or

$$Q = 2 \pi d_d k_{g_{ref}} (T_\infty - T_s) \frac{\ln(1 + B_M)}{B_M} \quad (2.35)$$

Now the heat used in vaporization of the fuel is

$$Q_e = \dot{m}_v L = 2 \pi d_d (k/C_p)_{g_{ref}} L \ln(1 + B_M) \quad (2.36)$$

So the heat available for the heating up the drop is obtained by the difference between Q and Q_e . Then we have

$$Q - Q_e = 2 \pi d_d k_{g_{ref}} \ln(1 + B_T) \left(\frac{T_\infty - T_s}{B_M} - \frac{L}{C_{pg_{ref}}} \right) \quad (2.37)$$

or

$$Q - Q_e = \dot{m}_v L \left(\frac{B_T}{B_M} - 1 \right) \quad (2.38)$$

It should be noted in Eq. 2.38 that when $B_T = B_M$ the value of $Q - Q_e$ becomes zero, denoting the end of the heat-up period.

2.7 Liquid Phase Analysis

Transport processes within the drop are treated in different ways by different models such as the thin skin model, uniform temperature model, uniform state model. In this study we will use the uniform temperature model also known as ‘rapid mixing limit’ or ‘infinite conductivity model’ which postulates infinite thermal diffusivity and assumes that the temperature within the droplet is spatially uniform although time varying. We also assume that the species concentration is uniform within the drop.

2.8 Convective effects on evaporation

For drop evaporation under quiescent conditions, the principal mode of heat transfer is conduction. But if relative motion exists between the droplet and the surrounding gas or air, the rate of evaporation is enhanced. The gas-phase convective environment has a considerable impact on the droplet evaporation process, as both the heat and the mass transfer process between the phases are enhanced by relative motion between them. In order to consider these phenomena, mass flux and energy transfer rates are corrected by implementing the semi-empirical correlations for the calculation of both mass and heat transfer numbers in the case of forced convection. One of the first reliable correlations was given by Frossling [11]. He showed that the effect of convection on heat and mass transfer rates could be accommodated by a correction factor that is a function of Reynolds number and Schmidt or Prandtl number.

The original correction factor has been later modified by Ranz and Marshall [12] to

$$1 + 0.3 Re_d^{0.5} Pr_g^{0.33} \quad (2.39)$$

Combining equations 2.28 and 2.39 yields the following equation for the rate of fuel evaporation under convective environment:

$$\dot{m}_v = 2\pi d_d \left(\frac{k}{C_p} \right)_{g_{ref}} \ln(1 + B_M) (1 + 0.3 Re_d^{0.5} Pr_g^{0.33}) \quad (2.40)$$

This equation gives the instantaneous rate of evaporation for a drop of diameter d_d . As described earlier heat transfer rates between the phases are also enhanced under convective environment. So the expression for rate of heat transferred from the gas to the drop Q (Eqn. 2.35) and the heat used in vaporization of the fuel Q_e (Eqn. 2.36) can also be modified using the correction factor as follows,

$$Q = 2\pi d_d k_{g_{ref}} (T_\infty - T_s) \frac{\ln(1 + B_M)}{B_M} (1 + 0.3 Re_d^{0.5} Pr_g^{0.33}) \quad (2.41)$$

and

$$Q_e = \dot{m}_v L = 2\pi d_d \left(\frac{k}{C_p} \right)_{g_{ref}} L \ln(1 + B_M) (1 + 0.3 Re_d^{0.5} Pr_g^{0.33}) \quad (2.42)$$

In the above expressions Re_d is the droplet Reynolds number. The definition of droplet Reynolds number is based on the relative velocity between the droplet and

the surrounding gas, on the free stream density and the average gas film viscosity. Eqns 2.40 through 2.42 are appropriate when heat transfer is the controlling process in evaporation. If however, mass transfer is the controlling mechanism we replace Pr_g by Schmidt number Sc_g in these equations.

2.9 Property Evaluation

In addition to the aforementioned assumptions, the classical D^2 -law also includes the assumption that the Lewis number within the gas phase is unity. The definition of the Lewis number, $Le \equiv \alpha/D_c$, it can be seen that $\alpha = D_c$ for the present case, where $\alpha = k/(\rho C_p)$ is the thermal diffusivity. This implies that the rate of heat and mass transfer are of the same magnitude. This assumption provide simplificationn and as a consequence, the number of properties which has to be evaluated in order to solve the problem is reduced. This is true only for the steady-state analysis. The properties such as density and thermal conductivity of the evaporated liquid has to be evaluated at some mean film temperature and composition. In the literature several schemes have been proposed but many authors found that the scheme which they called the ‘1/3 rule’ worked best. The rule used the following reference states for temperature and composition, designated with the subscript r:

$$T_r = T_S + \frac{T_\infty - T_S}{3} \quad (2.43)$$

$$Y_{F_r} = Y_{F_S} + \frac{Y_{F_\infty} - Y_{F_S}}{3} \quad (2.44)$$

where Y_F is mass fraction of the fuel vapour. Subscripts s and ∞ refer to the surface and ambient conditions. If the fuel concentration at an infinite distance from the droplet is assumed to be zero, equation 2.44 becomes

$$Y_{F_r} = \frac{2}{3} Y_{F_S} \quad (2.45)$$

and

$$Y_{A_r} = 1 - Y_{F_r} = 1 - \frac{2}{3} Y_{F_S} \quad (2.46)$$

where Y_{A_r} is the reference mass fraction of air.

The above equations are used in this study to calculate the reference values of the physical properties of the vapour-gas mixture that constitutes the environment of the evaporating drop. This means that the reference state is closer to the droplet surface than the mean film value. For example, the reference specific heat and thermal conductivity is obtained as,

$$C_{pg_{ref}} = Y_{A_r} (C_{pA} \text{ at } T_r) + Y_{F_r} (C_{pv} \text{ at } T_r) \quad (2.47)$$

$$k_{g_{ref}} = Y_{A_r} (k_A \text{ at } T_r) + Y_{F_r} (k_v \text{ at } T_r) \quad (2.48)$$

Chapter 3

Discretization Procedure and Solution Algorithm

3.1 Description of the Finite Volume Method

The Finite Volume method for solving the incompressible Navier Stokes equations has become very popular in recent years because of the following advantages

1. It is easy to implement on non-orthogonal curvilinear grids.
2. The solution can be obtained in the actual physical domain without transforming the governing equations.
3. It is easy to implement the boundary conditions.

When the primitive variable (e.g. velocity and pressure) approach is used, special treatment for pressure is required in the solution algorithm because the pressure does not have its own governing equation for incompressible flow. The continuity equation, having no explicit link to the pressure, is just an additional constraint on the velocity field that must be satisfied together with the momentum equations. The appropriate manipulation of this constraint leads to an equation for the pressure.

In the present study, the Navier Stokes and Energy equations have been solved using the finite volume method. We have used non-staggered (collocated) grid arrangement, where the dependent variables are calculated at the centroid of the finite volume cells. But this arrangement can produce non-physical oscillations

in the pressure field, the so-called checker-board pressure distribution. When central differencing is used to represent both the pressure gradient term in the momentum equations and the cell-face velocity in the continuity equation, it then happens that the velocities depend on pressure at alternate nodes and not on adjacent ones and the pressure too depends on velocities at alternate nodes. This behavior is called velocity-pressure decoupling, Patankar [50].

To avoid this decoupling, the momentum interpolation method, first proposed by Rhie and Chow [52] has been used. In this approach, the cell-face velocity in the continuity equations are evaluated by linearly interpolating the so-called “mass” velocities computed without the pressure terms in the discretized equations while directly evaluating the pressure gradient using values at the adjacent cell centers. This results in a strong velocity-pressure coupling. The pressure gradient terms, appearing in the momentum equations, are still represented by central difference approximation.

3.2 Integral Form of Governing Equations

The three-dimensional Navier-Stokes equations can be expressed in the following general convection-diffusion-source integral form:

$$\frac{\partial}{\partial t} \int_V \rho dV + \int_S \rho \mathbf{u} \cdot \mathbf{dS} = 0 \quad (3.1)$$

$$\frac{\partial}{\partial t} \int_V \rho \phi dV + \int_S [\rho \mathbf{u} \phi - \Gamma_\phi \nabla \phi] \cdot \mathbf{dS} = \int_V S_\phi dV \quad (3.2)$$

where ρ represents the fluid density, \mathbf{u} is the fluid velocity, Γ_ϕ is the diffusion coefficient for the quantity ϕ (viscosity in case of momentum equations), ϕ stands for any vector component or scalar quantity, S_ϕ is the volumetric source term. If ϕ is other than velocity *i.e* temperature, scalar *etc.* then density (ρ) should be replaced by $(\rho C_p)_\phi$.

In this formulation we work with **Cartesian components** of velocity. So ϕ can be the three Cartesian component of velocity u, v, w as well as any scalar *e.g.*, temperature, species concentration, which needs to be determined.

3.3 FVM for 3-D Geometry

We will now discuss the finite volume method applied to a general 3-D geometry. The entire solution domain is initially divided into zones and then zones are subdivided into a number of finite volumes defined by the coordinates of their eight vertices. We have used the collocated grid arrangement where all the dependent variables are defined at the centroid of the cell. The calculation of surface vectors for each of the face of the finite volume and also its volume is explained in detail by Narasimha [49] and [40]. These computations are done in the manner suggested by Kordulla and Vinokur [46].

3.4 Discretization Procedure

The discretization of the transport equations is performed using the finite volume approach. All the transport equation can be represented in the following general form,

$$\frac{\partial}{\partial t} \int_V \rho \phi dV + \int_S [\rho \mathbf{u} \phi - \Gamma_\phi \nabla \phi] \cdot \mathbf{dS} = \int_V S_\phi dV \quad (3.3)$$

which consists of the rate of change of ϕ , convection diffusion fluxes and the source term. The rate of change and source terms are integrated over the cell volume, whereas the convection and diffusion terms is summed through the CV faces.

3.4.1 Discretization of the General Convection-Diffusion Equation

(a) Rate of change: In the discretization of the unsteady term it has been assumed that the value of the dependent variable at the centroid is the average over the entire control volume. Thus

$$\frac{\partial}{\partial t} \int_V \rho \phi dV \approx \frac{(\rho \phi V)_P^{n+1} - (\rho \phi V)_P^n}{\Delta t} \approx V_P \frac{(\rho \phi)_P^{n+1} - (\rho \phi)_P^n}{\Delta t} \quad (3.4)$$

where V_P is the volume of the cell.

(b) Convection fluxes: The approximation of the surface integral over convection flux of variable ϕ has been done in the following way,

$$\int_S \rho \mathbf{u} \phi \cdot d\mathbf{S} \approx \sum_j \rho_j \phi_j (\mathbf{u} \cdot \mathbf{S})_j = \sum F_j \phi_j \quad (3.5)$$

where ϕ_j is the value of ϕ at the center of the face j .

The value of the ϕ_j can be evaluated using either upwind scheme or central difference scheme.

The upwind scheme is based on the assumption that the convected cell face value is equal to that at the upstream cell along the same coordinate direction. Thus, the value ϕ_e at the east face is assigned the value ϕ_P if $u_e \geq 0$, *i.e.*, the flux F_e is positive, and the value ϕ_E if $u_e < 0$, *i.e.*, the flux F_e is negative. This can be conveniently summarized as

$$F_e \phi_e = \phi_P [|F_e, 0|] - \phi_E [| -F_e, 0|] \quad (3.6)$$

Here $[[p, q]]$ denotes the maximum of p and q . Similar expression can be written for the rest of the faces. While using central difference scheme, the value of ϕ_j is determined as,

$$F_e \phi_e = F_e \left(\frac{\overline{eE}}{\overline{PE}} \phi_P + \left(1 - \frac{\overline{eE}}{\overline{PE}}\right) \phi_E \right) \quad (3.7)$$

where, \overline{eE} is the distance between face and cell center E and \overline{PE} is the distance between cell centers.

(c) Diffusion fluxes: The surface integral over diffusion flux of variable ϕ can be approximated as

$$\int_S \Gamma_\phi \nabla \phi \cdot d\mathbf{S} \approx \sum_{j=e,w,n,s,t,b} (\Gamma_\phi \nabla \phi \cdot \mathbf{S})_j = \sum_j -F_j^d \quad (3.8)$$

For east face we can write,

$$F_e^d = -\Gamma_\phi \left(\alpha_1 \frac{\phi_E - \phi_P}{\Delta x^1} + \alpha_2 \frac{\phi_{se} - \phi_{ne}}{\Delta x^2} + \alpha_3 \frac{\phi_{te} - \phi_{be}}{\Delta x^3} \right) \quad (3.9)$$

Calculation of $\alpha_1, \alpha_2, \alpha_3$, the edge center values appearing in cross derivative diffusion flux, special treatment of diffusion fluxes of corner cells and computation of spatial derivatives at cell-center of a non-orthogonal grid is elaborated in Narasimha [49].

(d) **Source:** The source term is integrated over the cell volume as follows:

$$\int_V S_\phi dV \approx (S_\phi)_P V_P \quad (3.10)$$

In the momentum equations, the pressure term is a source term, while in species transport equations chemical reaction could be a source term.

(e) **Pressure Term:** Its discretization is same as that of the ordinary diffusion flux and is given by

$$-\int_{V_P} \nabla p \mathbf{n}_i dV \approx -(\nabla p \cdot \mathbf{n}_i)_P V_P \quad (3.11)$$

where \mathbf{n}_i is the unit vector in the direction of the velocity component, u_i . However, the Gauss divergence theorem can be used to convert the volume integral to a surface integral which can be discretized as

$$-\int_S p \mathbf{n}_i d\mathbf{S} \approx -\sum_j p_j S_{ij} \quad (3.12)$$

p_j is the pressure at the j^{th} face center and S_{ij} is the i^{th} direction component of the surface vector for face j .

3.5 The Discretized Equations

3.5.1 The Gas Phase

The discretized equations for the gas phase are

Continuity:

$$\Delta V_p \frac{\rho_g^{n+1} - \rho_g^n}{\Delta t} + \sum_f \rho_{gf}^{n+1} F_{gf}^{n+1} = \frac{1}{\vartheta_g} \Delta V_p A^n \quad (3.13)$$

Momentum:

$$\begin{aligned} \Delta V_p \frac{u_g^{n+1} - u_g^n}{\Delta t} + \sum_f u_{gf}^m F_{gf}^m + \frac{1}{\rho_g^n} \sum_f F_{duf}^{n+1} &= \frac{-1}{\rho_g^n} \sum_f P_f^{n+1} S_{fx} - \frac{\Delta V_p}{\vartheta_g \rho_g^n} A^n u_g^{n+1} \\ &+ \frac{\Delta V_p}{\vartheta_g \rho_g^n} (A^n u_d^n - \vartheta_d^n f_{dx}^n) + \Delta V_p g_x + u_g^n \sum_f F_{gf}^m \end{aligned} \quad (3.14)$$

$$\begin{aligned} \Delta V_p \frac{v_g^{n+1} - v_g^n}{\Delta t} + \sum_f v_{gf}^m F_{gf}^m + \frac{1}{\rho_g^n} \sum_f F_{dvwf}^{n+1} = \frac{-1}{\rho_g^n} \sum_f F_f^{n+1} S_{fy} - \frac{\Delta V_p}{\vartheta_g^n \rho_g^n} A^n v_g^{n+1} \\ + \frac{\Delta V_p}{\vartheta_g^n \rho_g^n} (A^n v_d^n - \vartheta_d^n f_{dy}^n) + \Delta V_p g_y + v_g^n \sum_f F_{gf}^m \end{aligned} \quad (3.15)$$

$$\begin{aligned} \Delta V_p \frac{w_g^{n+1} - w_g^n}{\Delta t} + \sum_f w_{gf}^m F_{gf}^m + \frac{1}{\rho_g^n} \sum_f F_{dvwf}^{n+1} = \frac{-1}{\rho_g^n} \sum_f F_f^{n+1} S_{fz} - \frac{\Delta V_p}{\vartheta_g^n \rho_g^n} A^n w_g^{n+1} \\ + \frac{\Delta V_p}{\vartheta_g^n \rho_g^n} (A^n w_d^n - \vartheta_d^n f_{dz}^n) + \Delta V_p g_z + w_g^n \sum_f F_{gf}^m \end{aligned} \quad (3.16)$$

Energy:

$$\begin{aligned} \Delta V_p C_{pg} \frac{T_g^{n+1} - T_g^n}{\Delta t} + \sum_f C_{pgf} T_{gf}^{n+1} F_{gf}^{n+1} + \frac{1}{\rho_g^{n+1}} \sum_f F_{dTf}^{n+1} = -\frac{\Delta V_p}{\vartheta_g^{n+1} \rho_g^{n+1}} A^n C_{vd} T_g^{n+1} \\ + \frac{\Delta V_p}{\vartheta_g^{n+1} \rho_g^{n+1}} A^n C_{vd} T_d^{n+1} - \frac{\Delta V_p}{\vartheta_g^{n+1} \rho_g^{n+1}} n^n Q^n + C_{pg} T_g^n \sum_f F_{gf}^{n+1} \end{aligned} \quad (3.17)$$

Fuel Mass Fraction:

$$\begin{aligned} \Delta V_p \frac{Y_F^{n+1} - Y_F^n}{\Delta t} + \sum_f Y_F^{n+1} F_{gf}^{n+1} + \frac{1}{\rho_g^{n+1}} \sum_f F_{dYf}^{n+1} = -\frac{\Delta V_p}{\vartheta_g^{n+1} \rho_g^{n+1}} A^n Y_F^{n+1} \\ + \frac{\Delta V_p}{\vartheta_g^{n+1} \rho_g^{n+1}} A^n + Y_F^n \sum_f F_{gf}^{n+1} \end{aligned} \quad (3.18)$$

In the equations 3.14 through 3.16, $m = n + 1$ for a fully implicit method and $m = n$ for a semi-implicit method. In the above equations, ΔV_p is the volume of the Finite Volume cell, u_g, v_g, w_g are the components of the gas phase velocity, u_d, v_d, w_d are the components of the droplet phase velocity, g_x, g_y, g_z are the components of acceleration due to gravity in X,Y, and Z directions respectively, $A^n = n^n \dot{m}_v^n$ and

$$F_{gf} = \mathbf{u}_{gf} \cdot \mathbf{S}_f$$

is the volume flux for the fluid phase, where

$$F_{d\phi f} = -\mu \nabla \phi_{gf} \cdot \mathbf{S}_f; \quad F_{dTf} = -k_{gf} \nabla T_{gf} \cdot \mathbf{S}_f$$

and

$$F_{dYf} = -(\rho_g D) \nabla Y_F \cdot \mathbf{S}_f$$

are the diffusion flux for the fluid ($\phi = u, v, w$), diffusion flux for temperature and mass fraction respectively. Note that in the energy equation the value of C_{pg} is lagged by one time step.

3.5.2 The Droplet Phase

The discretized equations for the droplet phase are

Continuity:

$$\Delta V_p \frac{\Theta_d^{n+1} - \Theta_d^n}{\Delta t} + \sum_f \Theta_{df}^{n+1} F_{df}^{n+1} = -\frac{\Delta V_p}{\rho_d \vartheta_0} A^n \quad (3.19)$$

Momentum:

$$\begin{aligned} \Delta V_p \frac{u_d^{n+1} - u_d^n}{\Delta t} + \sum_f u_{df}^m F_{df}^m &= \frac{-1}{\rho_d^n} \sum_f P_f^{n+1} S_{fx} + \Delta V_p g_x \\ &+ \frac{\Delta V_p}{\rho_d^n} f_{dx}^n + u_d^n \sum_f F_{df}^m \end{aligned} \quad (3.20)$$

$$\begin{aligned} \Delta V_p \frac{v_d^{n+1} - v_d^n}{\Delta t} + \sum_f v_{df}^m F_{df}^m &= \frac{-1}{\rho_d^n} \sum_f P_f^{n+1} S_{fy} + \Delta V_p g_y \\ &+ \frac{\Delta V_p}{\rho_d^n} f_{dy}^n + v_d^n \sum_f F_{df}^m \end{aligned} \quad (3.21)$$

$$\begin{aligned} \Delta V_p \frac{w_d^{n+1} - w_d^n}{\Delta t} + \sum_f w_{df}^m F_{df}^m &= \frac{-1}{\rho_d^n} \sum_f P_f^{n+1} S_{fz} + \Delta V_p g_z \\ &+ \frac{\Delta V_p}{\rho_d^n} f_{dz}^n + w_d^n \sum_f F_{df}^m \end{aligned} \quad (3.22)$$

where $m = n + 1$ for a fully implicit method and $m = n$ for a semi-implicit method.

$$F_{df} = \mathbf{u}_{df} \cdot \mathbf{S}_f$$

Here, F_{df} is the convective flux for the droplet phase.

Energy:

$$\Delta V_p C_{ld} \frac{T_d^{n+1} - T_d^n}{\Delta t} + C_{ld} \sum_f T_{df}^{n+1} F_{df}^{n+1} = \frac{\Delta V_p}{\rho_d \vartheta_d^{n+1}} (n^n Q^n - A^n L) + C_{ld} T_d^n \sum_f F_{df}^{n+1} \quad (3.23)$$

3.6 The Solution Algorithm

We use a time-accurate time stepping method to solve the equations. The total evaporation rate is represented by the parameter A and is given by

$$A^n = n^n \dot{m}_v \quad (3.24)$$

Where \dot{m}_v is the rate of evaporation for a single droplet and has to be found from the evaporation model as described earlier. The number density of droplets, n is found for each cell by using the previous time step values of ϑ_d and d_d as

$$n^n = \frac{6\vartheta_d^n}{\pi d_d^3} \quad (3.25)$$

The diameter of the droplets are updated by using the previous time step normalized volume fraction values as follows,

$$d_d = d_0 (\Theta_d^n)^{1/3} \quad (3.26)$$

We then calculate the source term due to drag by calculating C_d and β for each cell and storing the final drag value f_d^n .

We use a fully implicit scheme for solving the momentum equations for the gas phase. Hence the discretized momentum equations become

$$\Delta V_p \frac{u_g^{n+1} - u_g^n}{\Delta t} + \sum_f u_{gf}^{n+1} F_{gf}^{n+1} + \frac{1}{\rho_g^n} \sum_f F_{duf}^{n+1} = \frac{-1}{\rho_g^n} \sum_f P_f^{n+1} S_{fx} - \frac{\Delta V_p}{\vartheta_g^n \rho_g^n} A^n u_g^{n+1} + C_v \frac{\Delta V_p}{\vartheta_g^n \rho_g^n} (A^n u_d^n - \vartheta_d^n f_{dx}^n) + \Delta V_p g_x + u_g^n \sum_f F_{gf}^{n+1} \quad (3.27)$$

$$\begin{aligned} \Delta V_p \frac{v_g^{n+1} - v_g^n}{\Delta t} + \sum_f v_{gf}^{n+1} F_{gf}^{n+1} + \frac{1}{\rho_g^n} \sum_f F_{dvf}^{n+1} &= \frac{-1}{\rho_g^n} \sum_f P_f^{n+1} S_{fy} - \frac{\Delta V_p}{\vartheta_g^n \rho_g^n} A^n v_g^{n+1} \\ &+ C_v \frac{\Delta V_p}{\vartheta_g^n \rho_g^n} (A^n v_d^n - \vartheta_d^n f_{dy}^n) + \Delta V_p g_y + v_g^n \sum_f F_{gf}^{n+1} \end{aligned} \quad (3.28)$$

$$\begin{aligned} \Delta V_p \frac{w_g^{n+1} - w_g^n}{\Delta t} + \sum_f w_{gf}^{n+1} F_{gf}^{n+1} + \frac{1}{\rho_g^n} \sum_f F_{dwf}^{n+1} &= \frac{-1}{\rho_g^n} \sum_f P_f^{n+1} S_{fz} - \frac{\Delta V_p}{\vartheta_g^n \rho_g^n} A^n w_g^{n+1} \\ &+ C_v \frac{\Delta V_p}{\vartheta_g^n \rho_g^n} (A^n w_d^n - \vartheta_d^n f_{dz}^n) + \Delta V_p g_z + w_g^n \sum_f F_{gf}^{n+1} \end{aligned} \quad (3.29)$$

We follow a two-step procedure to obtain the gas phase velocity components. The first step has two major loops - an inner loop (*) and an outer loop (**). In the inner loop, we first ignore the pressure completely and solve the Eqns.(3.27) through (3.29) for the so-called mass velocities u_g^* , v_g^* and w_g^* . The equations for mass velocity are

$$\begin{aligned} \Delta V_p \frac{u_g^* - u_g^n}{\Delta t} + \sum_f u_{gf}^* F_{gf}^{**} + \frac{1}{\rho_g^n} \sum_f F_{duf}^* &= -\frac{\Delta V_p}{\vartheta_g^n \rho_g^n} A^n u_g^* \\ &+ C_v \frac{\Delta V_p}{\vartheta_g^n \rho_g^n} (A^n u_d^n - \vartheta_d^n f_{dx}^n) + \Delta V_p g_x + u_g^n \sum_f F_{gf}^{**} \end{aligned} \quad (3.30)$$

$$\begin{aligned} \Delta V_p \frac{v_g^* - v_g^n}{\Delta t} + \sum_f v_{gf}^* F_{gf}^{**} + \frac{1}{\rho_g^n} \sum_f F_{dvf}^* &= -\frac{\Delta V_p}{\vartheta_g^n \rho_g^n} A^n v_g^* \\ &+ C_v \frac{\Delta V_p}{\vartheta_g^n \rho_g^n} (A^n v_d^n - \vartheta_d^n f_{dy}^n) + \Delta V_p g_x + u_g^n \sum_f F_{gf}^{**} \end{aligned} \quad (3.31)$$

$$\begin{aligned} \Delta V_p \frac{w_g^* - w_g^n}{\Delta t} + \sum_f w_{gf}^* F_{gf}^{**} + \frac{1}{\rho_g^n} \sum_f F_{dwf}^* &= -\frac{\Delta V_p}{\vartheta_g^n \rho_g^n} A^n w_g^* \\ &+ C_v \frac{\Delta V_p}{\vartheta_g^n \rho_g^n} (A^n w_d^n - \vartheta_d^n f_{dz}^n) + \Delta V_p g_x + u_g^n \sum_f F_{gf}^{**} \end{aligned} \quad (3.32)$$

Eqns.(3.30) through (3.32) are iterated to convergence within the inner loop. We use a superscript * for the diffusion term because the diffusion terms are calculated in terms of the mass velocities as they are being iterated in the inner

loop. The superscript ** used in the convective flux F_{gf} which is evaluated in the outer loop of the first step, and is kept unchanged during the inner loop (*) iterations.

We then follow the same procedure for the momentum equations of the droplet phase. Hence, we have the fully-implicit discretized momentum equations as

$$\Delta V_p \frac{u_d^{n+1} - u_d^n}{\Delta t} + \sum_f u_{df}^{n+1} F_{df}^{n+1} = \frac{-1}{\rho_d^n} \sum_f P_f^{n+1} S_{fx} + \Delta V_p g_x + \frac{\Delta V_p}{\rho_d^n} f_{dx}^n + u_d^n \sum_f F_{df}^{n+1} \quad (3.33)$$

$$\Delta V_p \frac{v_d^{n+1} - v_d^n}{\Delta t} + \sum_f v_{df}^{n+1} F_{df}^{n+1} = \frac{-1}{\rho_d^n} \sum_f P_f^{n+1} S_{fy} + \Delta V_p g_y + \frac{\Delta V_p}{\rho_d^n} f_{dy}^n + v_d^n \sum_f F_{df}^{n+1} \quad (3.34)$$

$$\Delta V_p \frac{w_d^{n+1} - w_d^n}{\Delta t} + \sum_f w_{df}^{n+1} F_{df}^{n+1} = \frac{-1}{\rho_d^n} \sum_f P_f^{n+1} S_{fz} + \Delta V_p g_z + \frac{\Delta V_p}{\rho_d^n} f_{dz}^n + w_d^n \sum_f F_{df}^{n+1} \quad (3.35)$$

The discretized mass velocity equations are

$$\Delta V_p \frac{u_d^* - u_d^n}{\Delta t} + \sum_f u_{df}^* F_{df}^{**} = \Delta V_p g_x + \frac{\Delta V_p}{\rho_d^n} f_{dx}^n + u_d^n \sum_f F_{df}^{**} \quad (3.36)$$

$$\Delta V_p \frac{v_d^* - v_d^n}{\Delta t} + \sum_f v_{df}^* F_{df}^{**} = \Delta V_p g_y + \frac{\Delta V_p}{\rho_d^n} f_{dy}^n + v_d^n \sum_f F_{df}^{**} \quad (3.37)$$

$$\Delta V_p \frac{w_d^* - w_d^n}{\Delta t} + \sum_f w_{df}^* F_{df}^{**} = \Delta V_p g_z + \frac{\Delta V_p}{\rho_d^n} f_{dz}^n + w_d^n \sum_f F_{df}^{**} \quad (3.38)$$

Eqns.(3.36) through (3.38) too are iterated to convergence in three separate subloops in the inner loop of the first step. During any pass through the droplet mass velocity loop, we hold the convective fluxes F_{df}^{**} fixed and iterate for the mass velocities. Once the gas and droplet mass velocities are obtained we update the pressure and the fluxes in the outer loop and return to the inner loop and use the updated fluxes for the next pass. This continues until the fluxes F_{gf}^{**} and F_{df}^{**} converge in the outer loop, and henceforth, taken as the final values, F_{gf}^{n+1} and F_{df}^{n+1} .

We now look into the outer loop calculations. Having obtained the tentative mass velocities we turn to the pressure Poisson equation. This is derived from total mass conservation principle. By adding Eqn.(2.1) and Eqn.(2.5), we get

$$\frac{\partial \vartheta_g \rho_g}{\partial t} + \nabla \cdot (\vartheta_g \rho_g \mathbf{u}_g) + \frac{\partial (\rho_d \vartheta_d)}{\partial t} + \nabla \cdot (\rho_d \vartheta_d \mathbf{u}_d) = 0 \quad (3.39)$$

For steady state problems, time derivative term can be neglected

$$\nabla \cdot (\vartheta_g \rho_g \mathbf{u}_g) + \nabla \cdot (\rho_d \vartheta_d \mathbf{u}_d) = 0 \quad (3.40)$$

This continuity equation should be applied at the $(n+1)^{th}$ time level. Hence, we get

$$\nabla \cdot (\vartheta_g \rho_g \mathbf{u}_g)^{n+1} + \nabla \cdot (\rho_d \vartheta_d \mathbf{u}_d)^{n+1} = 0 \quad (3.41)$$

By subtracting Eqn.(3.30) from Eqn.(3.27), Eqn.(3.31) from Eqn.(3.28) and Eqn.(3.32) from Eqn.(3.29), we get

$$u_g^{n+1} - u_g^* = \frac{\Delta t}{\rho_g} \nabla P \quad (3.42)$$

Similarly, for droplet phase

$$u_d^{n+1} - u_d^* = \frac{\Delta t}{\rho_d} \nabla P \quad (3.43)$$

By multiplying Eqn.(3.42) and Eqn.(3.43) by $\rho_g \vartheta_g$ and $\rho_d \vartheta_d$ respectively and substituting in Eqn.(3.41), we get

$$\Delta t \nabla^2 P = \nabla \cdot (\vartheta_g \rho_g \mathbf{u}_g^*) + \nabla \cdot (\rho_d \vartheta_d \mathbf{u}_d^*) \quad (3.44)$$

In the above equation, we have used the principle $\vartheta_g + \vartheta_d = 1$. Discretization of Eqn.(3.44) leads to

$$\sum_f P_f^{**} \cdot S_f = \frac{1}{\Delta t} \left(\sum_f \vartheta_g^n \rho_g^n \mathbf{u}_{gf}^* \cdot S_f + \sum_f \vartheta_d^n \rho_d^n \mathbf{u}_{df}^* \cdot S_f \right) \quad (3.45)$$

We can define the fluxes on the RHS of Eqn.(3.45) as

$$F_{M_{gf}}^{**} [= (\vartheta_{gf}^n \rho_{gf}^n \mathbf{u}_{gf}^*) \cdot S_f] = (\vartheta_{gf}^n \rho_{gf}^n) F_{gf}^{**} \quad (3.46)$$

$$F_{M_{df}}^{**} [= (\vartheta_{df}^n \rho_{df}^n \mathbf{u}_{df}^*) \cdot S_f] = (\vartheta_{df}^n \rho_{df}^n) F_{df}^{**} \quad (3.47)$$

Here the values of u_{gi}^* and u_{di}^* at the cell faces is obtained by a linear interpolation. The superscript $*$ is used for pressure because Eqn.(3.45) is now iterated to convergence in the outer loop of step one.

Having obtained the pressure field P^{**} from Eqn.(3.45), we update the fluxes F_{gf} and F_{df} using momentum interpolation

$$F_{gf}^{**} = \mathbf{u}_{gf}^* \cdot S_f - \frac{\Delta t}{\rho_g^n} \nabla P_f^{**} \cdot S_f \quad (3.48)$$

$$F_{df}^{**} = \mathbf{u}_{df}^* \cdot S_f - \frac{\Delta t}{\rho_d^n} \nabla P_f^{**} \cdot S_f \quad (3.49)$$

After updating the fluxes F_{gf}^{**} and F_{df}^{**} in the outer loop, we once again solve the inner loop for the mass velocities, followed by the pressure and update the fluxes. This cycle continues until the values of fluxes converge. At that point we accept that $F_{gf}^{n+1} = F_{gf}^{**}$, $F_{df}^{n+1} = F_{df}^{**}$, $P^{n+1} = P^{**}$. We now iterate the full momentum Eqns.(3.27) through (3.29) and Eqns.(3.33) through (3.35) to convergence. This last part comprises step two of the two-step algorithm. We now have the \mathbf{u}_g^{n+1} and \mathbf{u}_d^{n+1} values.

Also in the second step, we next iterate the continuity equation of the droplet phase to obtain the normalized volume fraction using F_{df}^{n+1} obtained from the converged \mathbf{u}_{df}^{n+1}

$$\Delta V_p \frac{\Theta_d^{n+1} - \Theta_d^n}{\Delta t} + \sum_f \Theta_{df}^{n+1} F_{df}^{n+1} = -C_v \frac{\Delta V_p}{\rho_d \vartheta_0} A^n \quad (3.50)$$

We next solve the continuity equation of gas phase for density using F_{gf}^{**} obtained from the converged \mathbf{u}_g^{n+1} . The discretized form is iterated to convergence.

$$\Delta V_p \frac{\rho_g^{n+1} - \rho_g^n}{\Delta t} + \sum_f \rho_{gf}^{n+1} F_{gf}^{n+1} = C_v \frac{\Delta V_p}{\vartheta_g^{n+1}} A^n \quad (3.51)$$

Next, we solve the droplet temperature equation by iterating to convergence.

$$\begin{aligned} \Delta V_p C_{ld} \frac{T_d^{n+1} - T_d^n}{\Delta t} + C_{ld} \sum_f T_{df}^{n+1} F_{df}^{n+1} = C_v \frac{\Delta V_p}{\rho_d \vartheta_d^{n+1}} (n^n Q^n - A^n L) \\ + C_{ld} T_d^n \sum_f F_{df}^{n+1} \end{aligned} \quad (3.52)$$

We then solve the mass fraction equation and the energy equation of the gaseous phase.

$$\begin{aligned} \Delta V_p \frac{Y_F^{n+1} - Y_F^n}{\Delta t} + \sum_f Y_F^{n+1} F_{gf}^{n+1} + \frac{1}{\rho_g^{n+1}} \sum_f F_{dYf}^{n+1} = -\frac{\Delta V_p}{\vartheta_g^{n+1} \rho_g^{n+1}} A^n Y_F^{n+1} \\ + C_v \frac{\Delta V_p}{\vartheta_g^{n+1} \rho_g^{n+1}} A^n + Y_F^n \sum_f F_{gf}^{n+1} \end{aligned} \quad (3.53)$$

$$\begin{aligned} \Delta V_p C_{pg} \frac{T_g^{n+1} - T_g^n}{\Delta t} + \sum_f C_{pgf} T_{gf}^{n+1} F_{gf}^{n+1} + \frac{1}{\rho_g^{n+1}} \sum_f F_{dTf}^{n+1} = \\ -\frac{\Delta V_p}{\vartheta_g^{n+1} \rho_g^{n+1}} A^n C_{vd} T_g^{n+1} + C_v \frac{\Delta V_p}{\vartheta_g^{n+1} \rho_g^{n+1}} A^n C_{vd} T_d^{n+1} \\ - C_v \frac{\Delta V_p}{\vartheta_g^{n+1} \rho_g^{n+1}} n^n Q^n + C_{pg} T_g^n \sum_f F_{gf}^{n+1} \end{aligned} \quad (3.54)$$

Note that the previous time step source term values are used in all the equations. The above steps are sequentially carried out at each time step. For all the equations of the droplet phase the convective terms are discretized by the first-order upwind scheme. This is specially helpful in avoiding negative or unphysical values of the volume fraction, however the inherent dissipation effects of the scheme reduces the sharp gradients in the solution.

3.7 Summary of the Algorithm

1. Initialize properties and fields for the carrier phase and the droplet phase, grids and other parameters.

2. Transfer $(n + 1)^{th}$ time level values to n^{th} time level for all the solvable variables like volume fraction, velocity, density, temperature for the gas phase and droplet phase, fuel mass fraction and pressure.
3. Compute and store all the source terms with the previous time step values. Compute d_d by

$$d_d = d_0(\Theta_d)^{1/3} \quad (3.55)$$

4. Solve for the mass velocity of the gas phase and droplet phase separately by iterating Eqns.(3.30) through (3.32) and (3.36) through (3.38) respectively with previous time step source term values.
5. Compute momentum fluxes, F_{Mgf}^{**} and F_{Mdf}^{**} using Eqn.(3.46) and Eqn.(3.47).
6. Solve for the pressure P by iterating Eqn.(3.45) to convergence.
7. Compute volume fluxes F_{gf}^{**} and F_{df}^{**} using Eqn.(3.48) and Eqn.(3.49).
8. Repeat steps 4 to 7 until F_{gf}^{**} and F_{df}^{**} converge.
9. Accept $P^{n+1} = P$, $F_g f^{n+1} = F_g f^{**}$ and $F_d f^{n+1} = F_d f$
10. Iterate the full momentum equations for gas phase Eqns.(3.27) through (3.29) and full momentum equations for droplet phase Eqns.(3.33) through (3.35) to convergence separately to obtain \mathbf{u}_g^{n+1} and \mathbf{u}_d^{n+1} , respectively.
11. Solve the continuity equation of droplet phase Eqn(3.50) for normalized volume fraction of droplet, Θ_d^{n+1} . The volume fraction of the droplet phase is found using the relation $\vartheta_d^{n+1} = \vartheta_0 * \Theta_d^{n+1}$. Volume fraction of gas phase is obtained by using the relation $\vartheta_g^{n+1} = 1 - \vartheta_d^{n+1}$.
12. Solve the continuity equation of gas Eqn.(3.51) for obtaining gas phase density, ρ_g^{n+1} .
13. Solve the energy equation for the droplet phase Eqn.(3.52) for droplet temperature T_d^{n+1} .
14. Solve the evaporated fuel vapour mass fraction Eqn.(3.53) to obtain Y_F^{n+1} .

15. Solve the gas-phase energy Eqn.(3.54) to obtain T_g^{n+1} .
16. If the stopping criterion for the time stepping is not met return to step 2 and repeat steps 2 through 15 for the next time step and march forward in time.

3.8 Limiter for Θ_d equation

If for a cell $\Theta_d < \epsilon$ ($\sim 1e4$) we put $A^n = 0$ and $C_v = 0$. Otherwise, put $C_v = 1$ and compute and store A using n^{th} level variable values by aforementioned relationship. The value of ϵ implies that we are not allowing the diameter of the droplet to fall below a certain value which depends on the droplet initial diameter and volume fraction. The value of C_v used in the equations becomes zero when the diameter of the droplet reaches this particular value. When $C_v = 0$, all the inter-phase mass, momentum and energy transfer terms go to zero resulting in only the convection of the smallest droplets.

Chapter 4

Results and Discussion

For validating OpenFOAM based solver for “dilute laminar gas-droplet flow with evaporation”, we considered to simulate some complete test cases, which are already solved using Anupravaha and validated with the FLUENT. The domain, shown in the Figure 4.1, where $H = 0.1\text{ m}$ and $L = 1.0\text{ m}$ is considered for all the five cases. Expressions for the variation of properties for liquid and vapour phase of n-heptane fuel are given in Appendix.A. Inlet conditions and the property values which are common for all the cases are shown in Table 4.1.

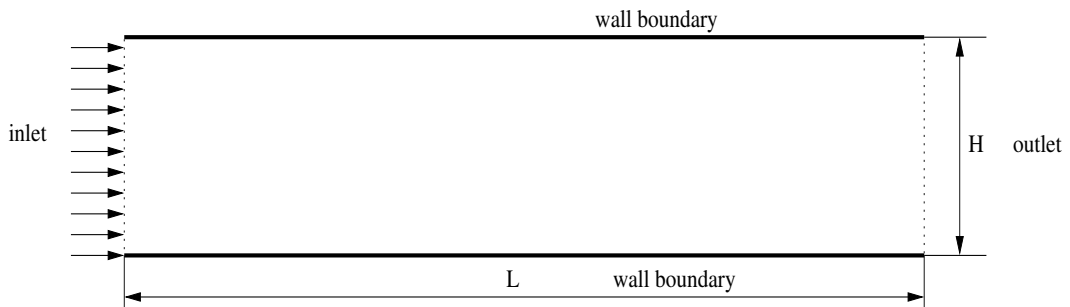


Figure 4.1: The Computational Domain for 2D-Channel Flow Problems

Table 4.1: Property values of fluids used

Property values	
Viscosity of gas	0.0000225 $N s/m^2$
Liquid droplet density, ρ_d	684.0 kg/m^3
Specific heat of air, C_{pa}	1006.43 $J/kg K$
Specific heat of fuel vapour, C_{vd}	2471.0 $J/kg K$
Specific heat of liquid droplet, C_{ld}	2219.0 $J/kg K$
Thermal conductivity of air, k_a	0.0242 $W/m K$
Thermal conductivity of fuel vapour, k_v	0.0128 $W/m K$
Latent heat of fuel, L	320096.0 J/kg
Mass diffusivity of vapour in gas, D	0.0000225 m^2/s

4.1 CASE 1: Gas-Droplet flow with $T_{di} = T_s$ and $u_{gi} = u_{di}$

In this case, both the gas phase and droplet phase enter the channel with a velocity of 1 m/s, when the inlet droplet temperature is equal to saturation temperature of n-heptane. The inlet properties are given in Table. 4.2.

Table 4.2: Case 1: Inlet Conditions

Inlet conditions	
Gas-phase inlet velocity	1.0 m/s
Droplet-phase inlet velocity	1.0 m/s
Inlet gas temperature	773.0 K
Inlet gas temperature	347.8 K
Inlet fuel mass fraction	0.0
Gas-phase inlet density	1.225 kg/m^3
Inlet volume fraction	0.0005
Droplet inlet diameter	50 μm

At the wall, homogegeous Neumann boundary condition is applied for the droplet-phase velocity and gas temperature for friction-less and insulated walls. Since, the droplet inlet temperature is equal to its saturation temperature, no transient heating will take place. Droplet remains at its inlet saturation temperature while evaporation happens due to heating from the gaseous phase. The gas temperature drops along the length of the channel giving heat to the droplets, which in turn

gets used for the evaporation and reaches a constant. But the evaporated fuel mass fraction and gaseous phase density increases due to the addition of vapour from droplets to gas because of evaporation.

The variation of different parameters along the length of the channel is plotted and compared with solver, Anupravaha and FLUENT. Results are having a slight difference from that of the FLUENT mainly because of the value of diameter used for drag calculations. In our solver, droplet diameter value (which changes owing to evaporation) is updated for the drag force calculation at each time step while in FLUENT, droplet diameter value remains same equal to its inlet value. Method for the calculation of values of properties is different in our solver from that of the FLUENT which causes some variation in results, especially in gas temperature, fuel mass fraction and gas density values. In addition to this, OpenFOAM and Anupravaha stops computing beyond a lesser value of droplet volume fraction due to the numerical difficulty caused by smaller diameter wherein FLUENT, there is no limit for it.

The variation of different flow variables and its comparison along the length of the channel are shown in Fig.4.5 to Fig.4.7. Contours for variables are plotted in figures from 4.2 to 4.4.

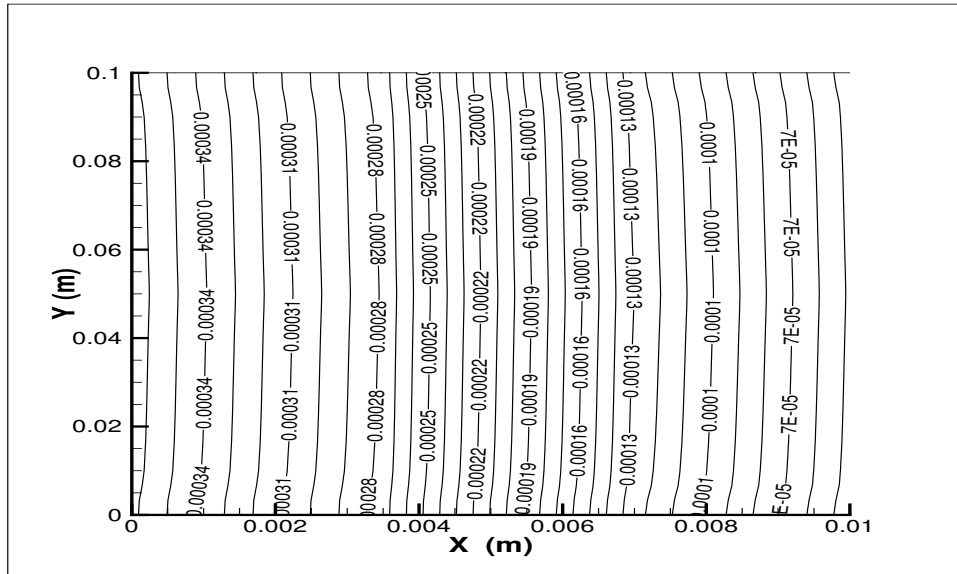
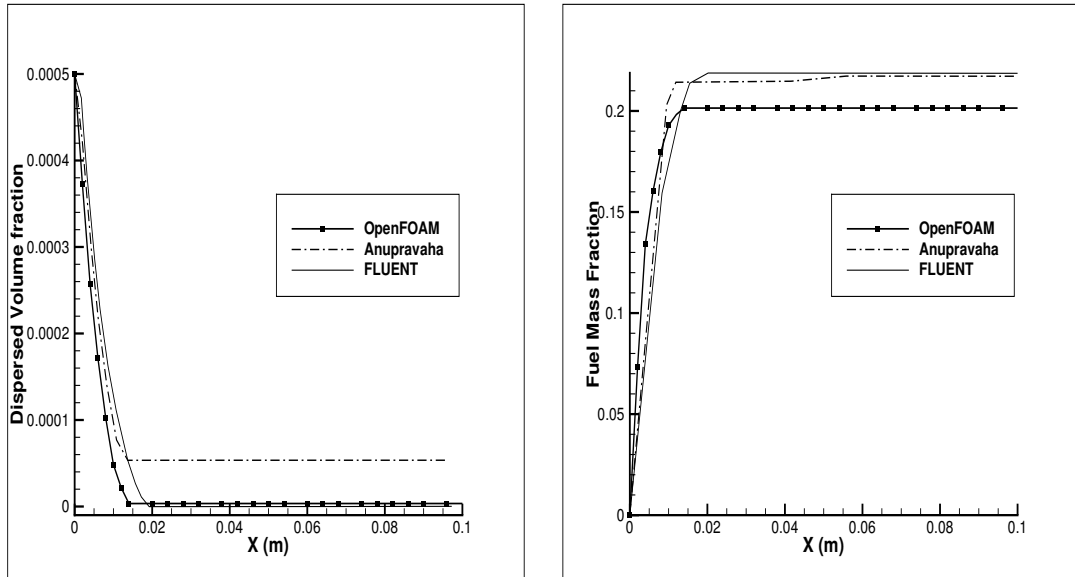
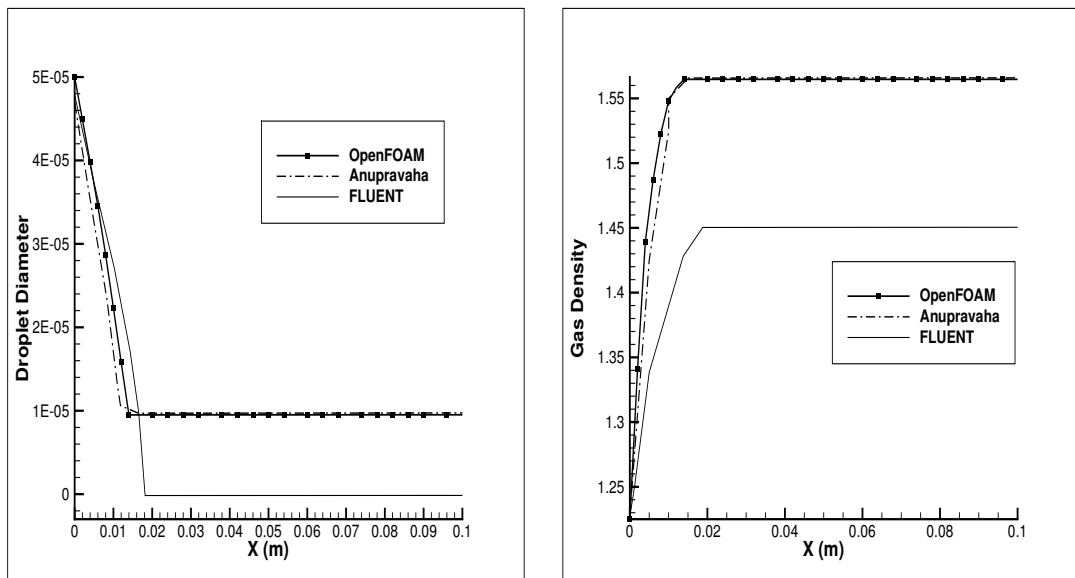


Figure 4.2: Case 1: Contour plot for droplet volume fraction



(a) Case 1: Droplet volume fraction (b) Case 1: Evaporated fuel mass fraction

Figure 4.5: Case 1: Variation along the length of the channel



(a) Case 1: Droplet Diameter(in m) (b) Case 1: Gas Density (in kg/m^3)

Figure 4.6: Case 1: Variation along the length of the channel

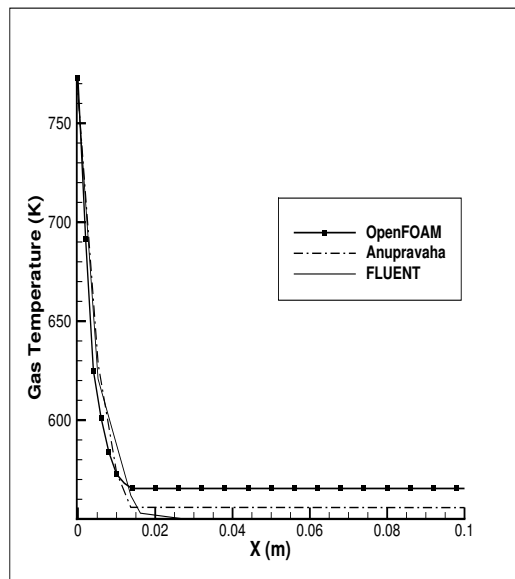


Figure 4.7: Case 1: Variation of Gas Temperature (in K) along the length of the channel

4.2 CASE 2: Gas-Droplet flow with $T_{di} = T_s$ and $u_{gi} > u_{di}$

For this case, gas phase moves with more velocity than that of droplet phase, when the inlet droplet temperature is equal to saturation temperature of n-heptane. The inlet properties are given in Table. 4.3. All other boundary conditions are same as that of Case 1. The droplets acquire gas velocity very quickly. Gaseous phase temperature variation differs from Case 1 as mass flow rate of gas-phase is double as that of Case 1. The property variation graphs and contour plots are shown in Fig.4.11 to Fig.4.12 and Fig.4.8 to Fig.4.10 respectively.

Table 4.3: Case 2: Inlet Conditions

Inlet conditions	
Gas-phase inlet velocity	2.0 <i>m/s</i>
Droplet-phase inlet velocity	1.0 <i>m/s</i>
Inlet gas temperature	773.0 <i>K</i>
Inlet gas temperature	347.8 <i>K</i>
Inlet fuel mass fraction	0.0
Gas-phase inlet density	1.225 <i>kg/m³</i>
Inlet volume fraction	0.0005
Droplet inlet diameter	50 μm

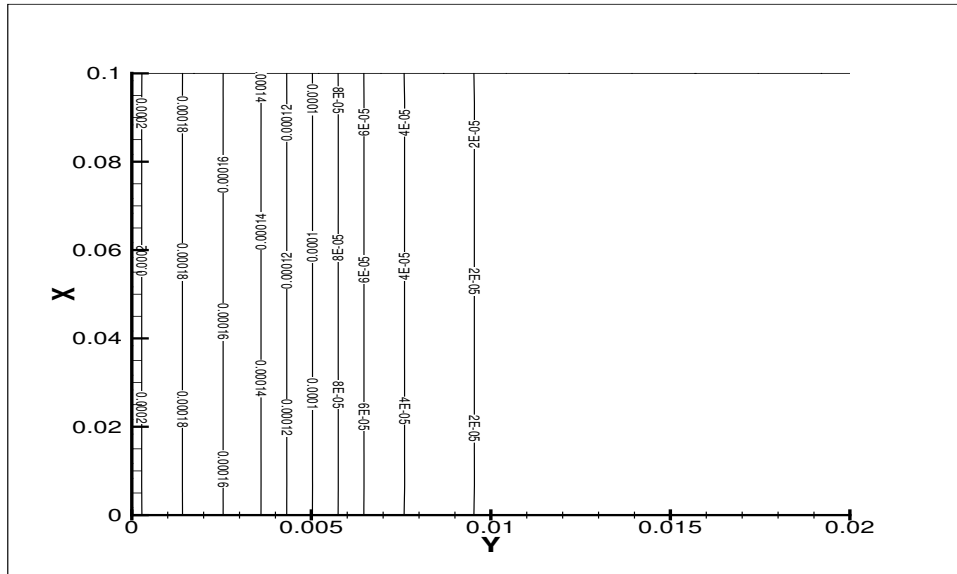


Figure 4.8: Case 2: Contour plot for droplet volume fraction

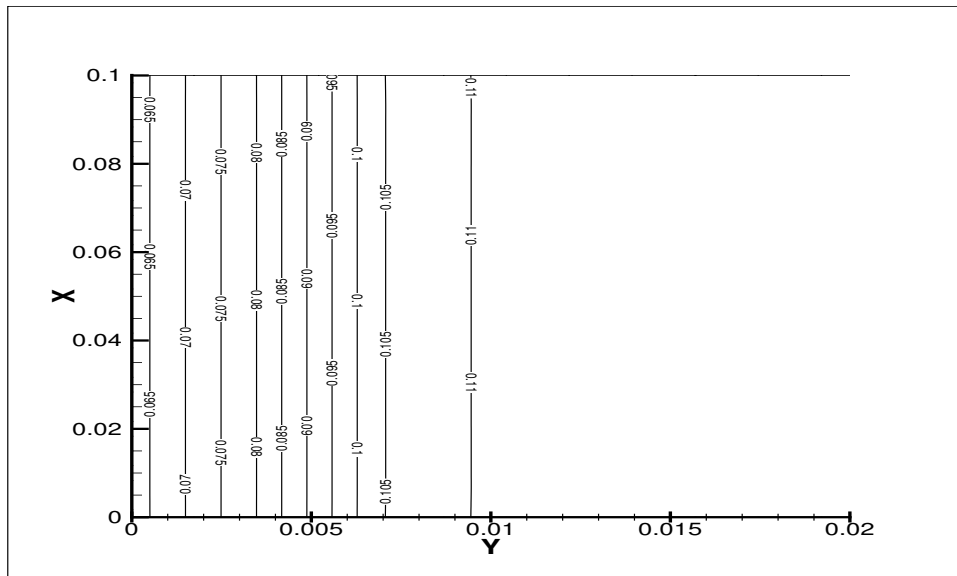


Figure 4.9: Case 2: Contour plot for evaporated fuel mass fraction

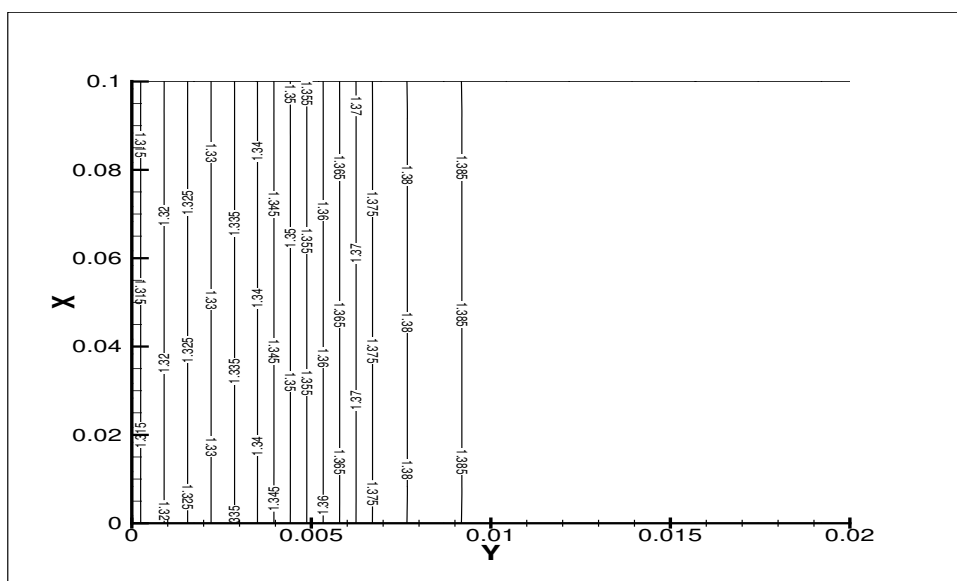
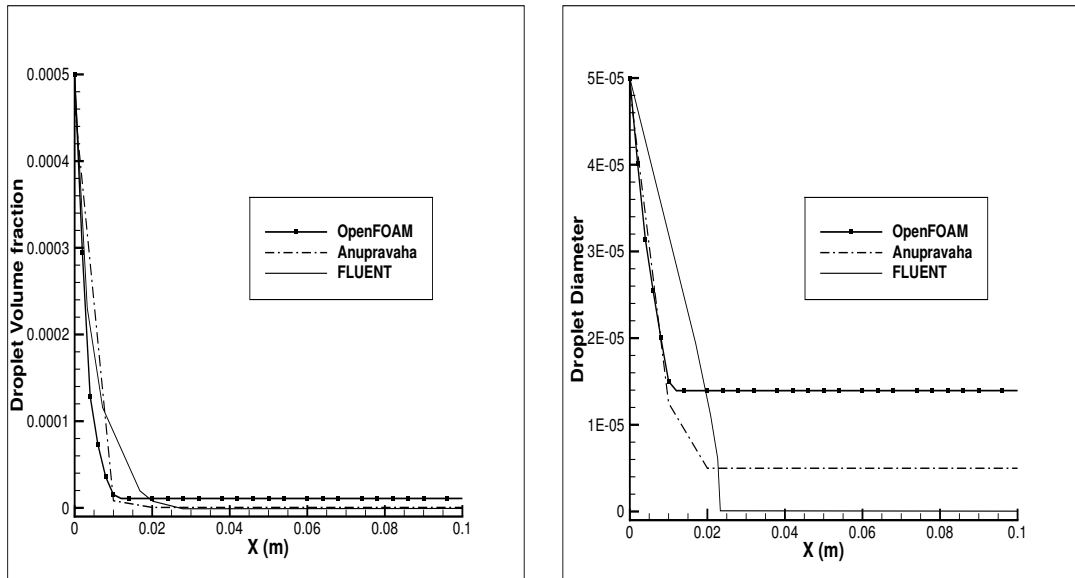


Figure 4.10: Case 2: Contour plot for gas density (in kg/m^3)



(a) Case 2: Droplet volume fraction

(b) Case 2: Droplet Diameter(in m)

Figure 4.11: Case 2: Variation along the length of the channel

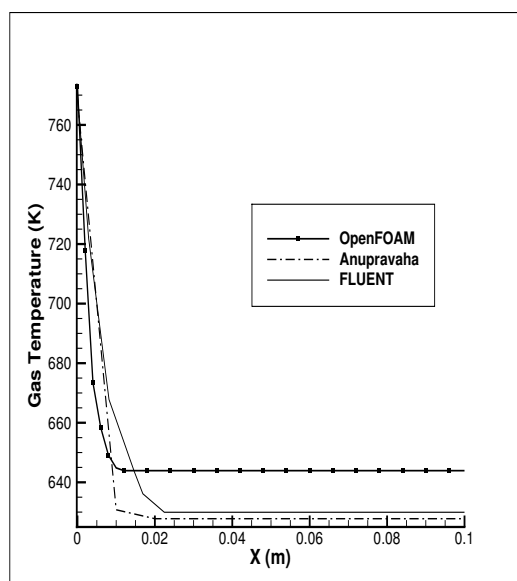


Figure 4.12: Case 2: Variation of Gas Temperature (in K) along the length of the channel

4.3 CASE 3: Gas-Droplet flow with $T_{di} = T_s$ and $u_{gi} < u_{di}$

In this case, gas phase moves with less velocity than that of droplet phase, when the inlet droplet temperature is equal to saturation temperature of n-heptane. The inlet properties are given in Table.4.4. In this case, droplets decelerate quickly and attain the gaseous phase velocity. Fraction of fuel evaporated increases compared to both previous cases as droplets residence time increases because of its lesser velocity. All plots (contour and comparison curves) of this case is shown in figures from Fig.4.13 to Fig.4.17.

Table 4.4: Case 3: Inlet Conditions

Inlet conditions	
Gas-phase inlet velocity	0.5 m/s
Droplet-phase inlet velocity	1.0 m/s
Inlet gas temperature	773.0 K
Inlet gas temperature	347.8 K
Inlet fuel mass fraction	0.0
Gas-phase inlet density	1.225 kg/m ³
Inlet volume fraction	0.0005
Droplet inlet diameter	50 μ m

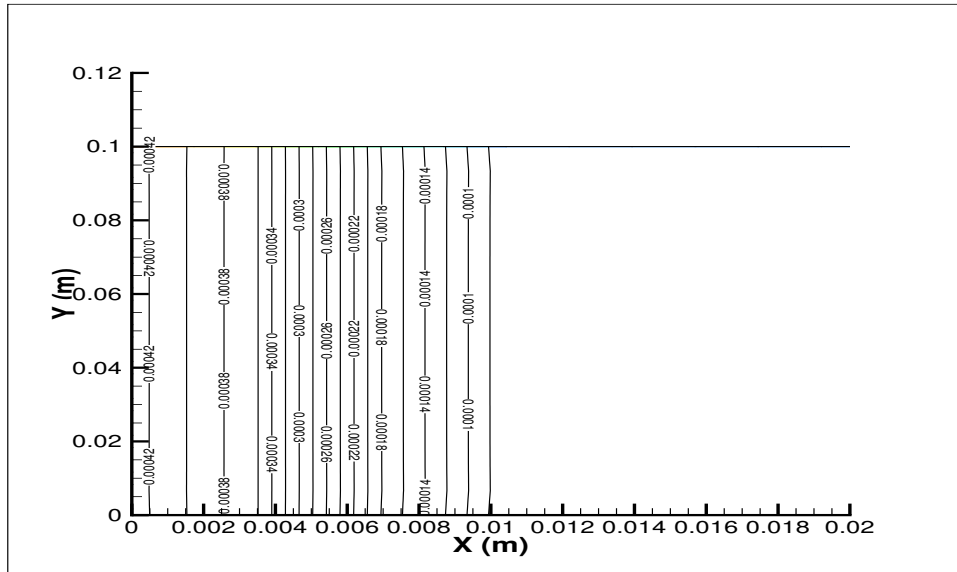


Figure 4.13: Case 3: Contour plot for droplet volume fraction

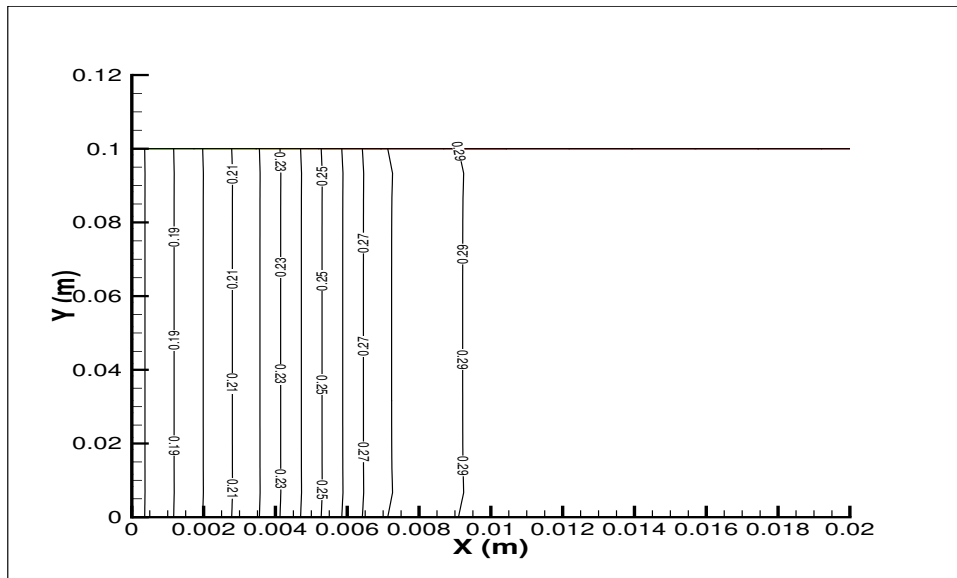


Figure 4.14: Case 3: Contour plot for evaporated fuel mass fraction

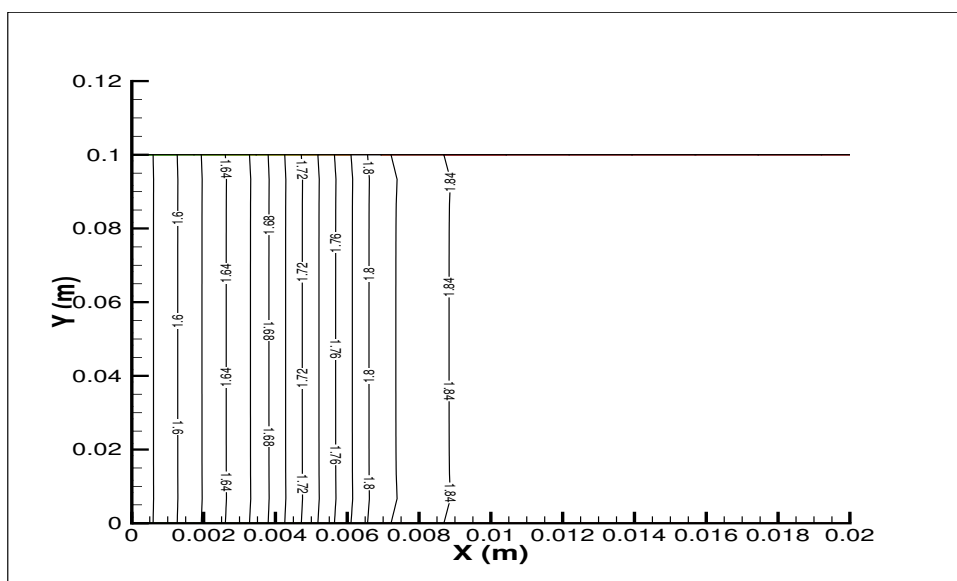


Figure 4.15: Case 3: Contour plot for gas density (in kg/m^3)

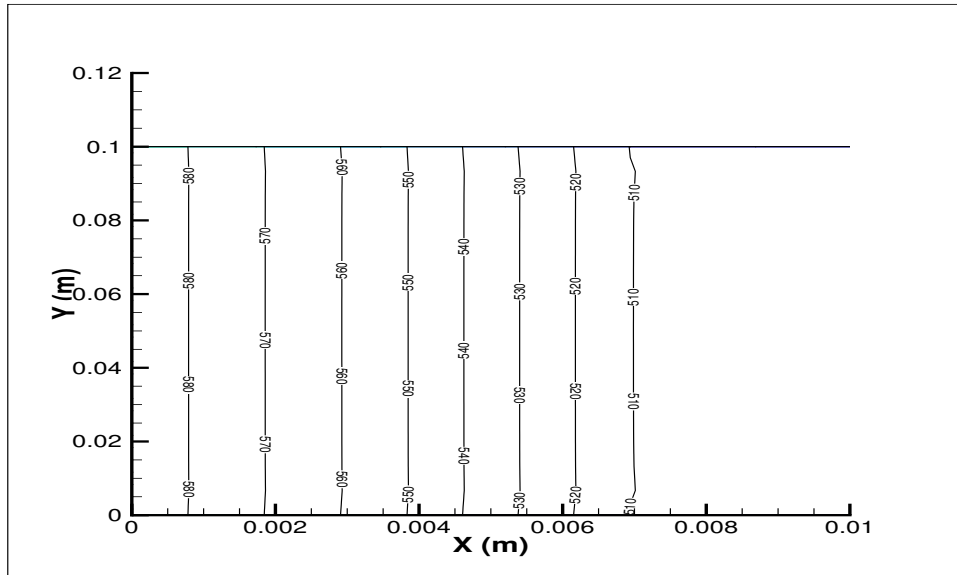
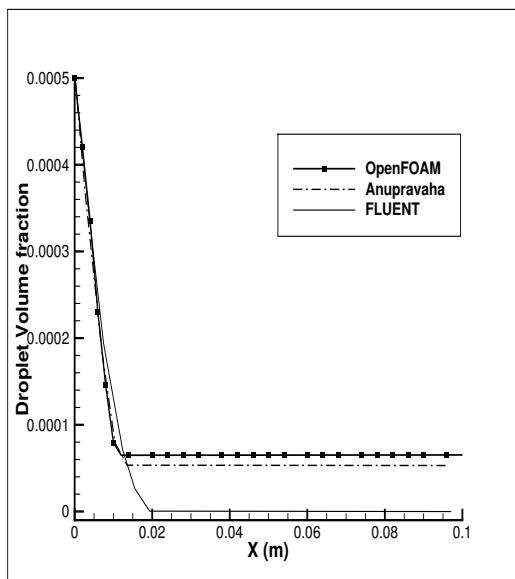
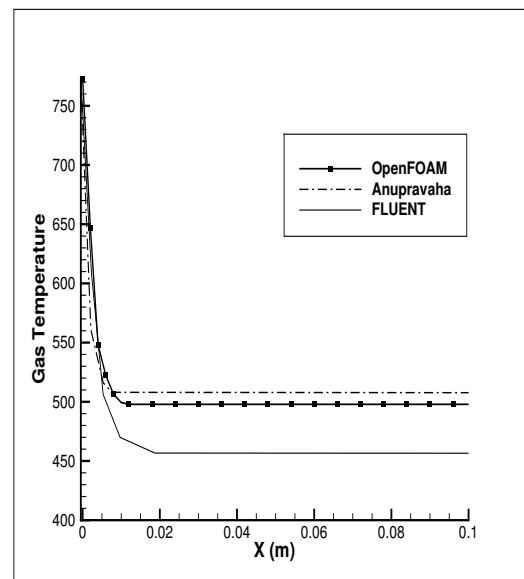


Figure 4.16: Case 3: Contour plot for gas temperature (in K)



(a) Case 3: Droplet volume fraction



(b) Case 3: Gas Temperature (in K)

Figure 4.17: Case 3: Variation along the length of the channel

4.4 CASE 4: Gas-Droplet flow with $T_{di} < T_s$ and $u_{gi} = u_{di}$

In this case, both the gas phase and droplet phase enter the channel with a velocity of 1 m/s, when the inlet droplet temperature is less than the saturation temperature of n-heptane. The inlet properties are given in Table. 4.5. In this case droplet temperature varies till it reaches its saturation value. Contour plots and comparison graphs which are having slight difference from the previous cases are shown in Fig.4.18 to Fig.4.23.

Table 4.5: Case 4: Inlet Conditions

Inlet conditions	
Gas-phase inlet velocity	1.0 m/s
Droplet-phase inlet velocity	1.0 m/s
Inlet gas temperature	773.0 K
Inlet gas temperature	300.0 K
Inlet fuel mass fraction	0.0
Gas-phase inlet density	1.225 kg/m ³
Inlet volume fraction	0.0005
Droplet inlet diameter	50 μ m

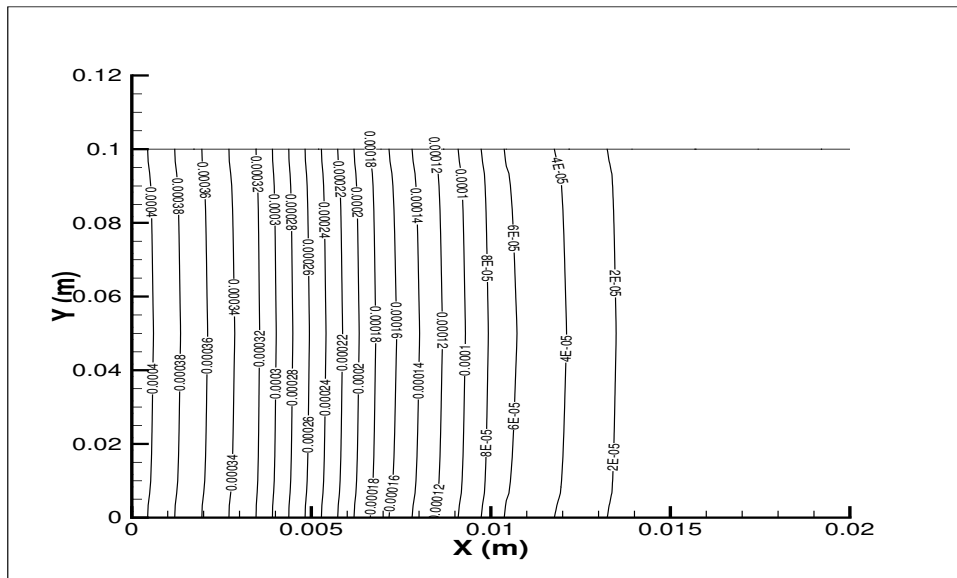


Figure 4.18: Case 4: Contour plot for droplet volume fraction

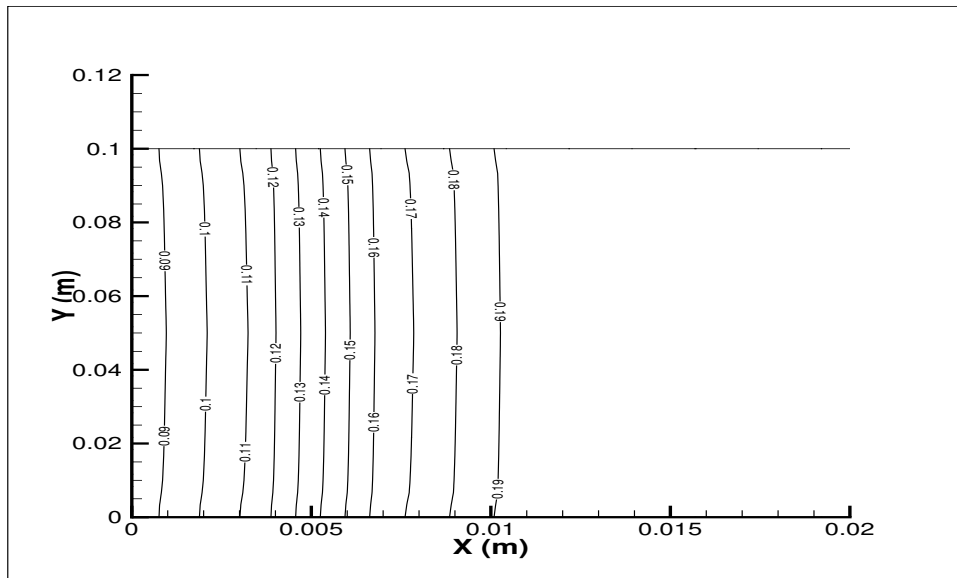


Figure 4.19: Case 4: Contour plot for evaporated fuel mass fraction

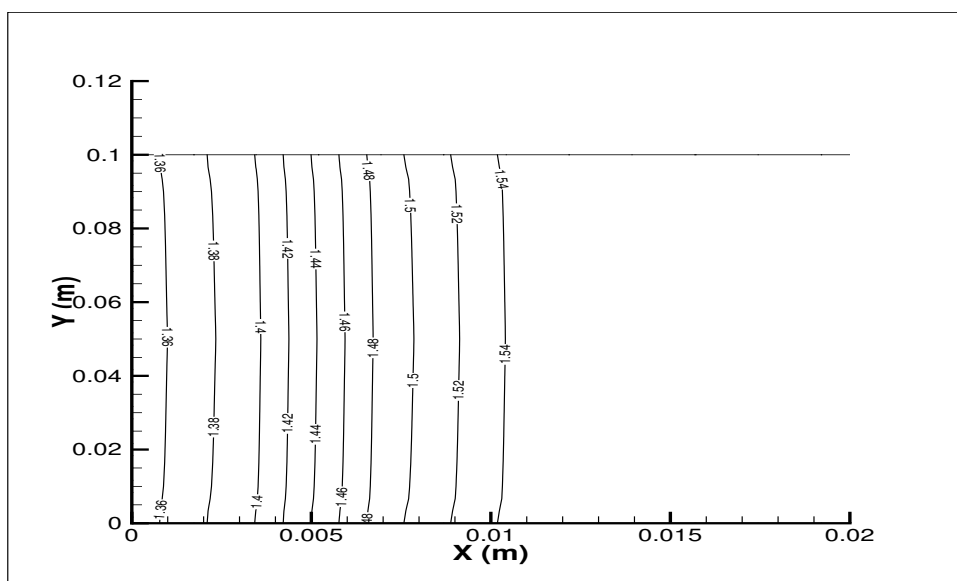


Figure 4.20: Case 4: Contour plot for gas density (in kg/m^3)

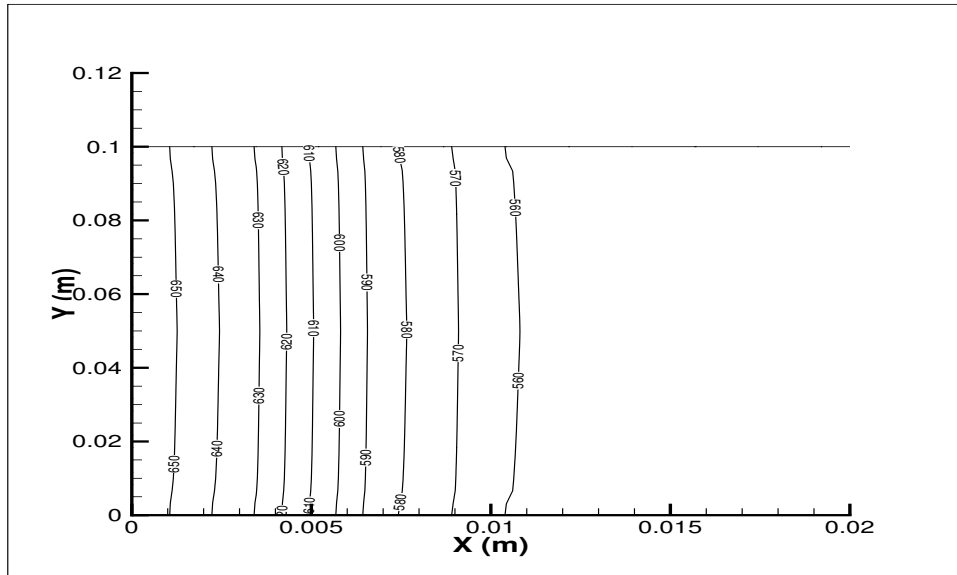


Figure 4.21: Case 4: Contour plot for gas temperature (in K)

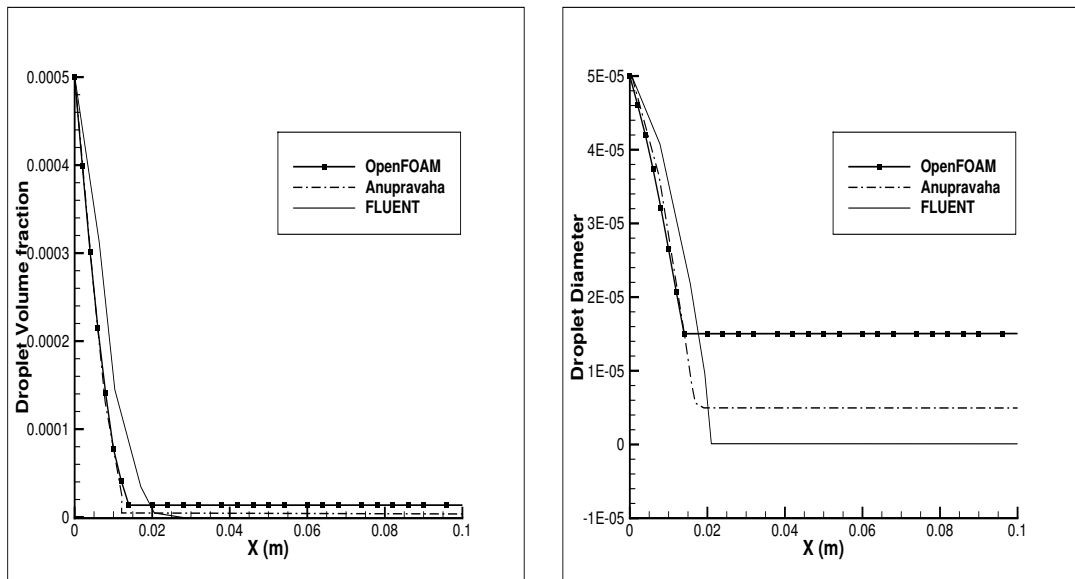


Figure 4.22: Case 4: Variation along the length of the channel

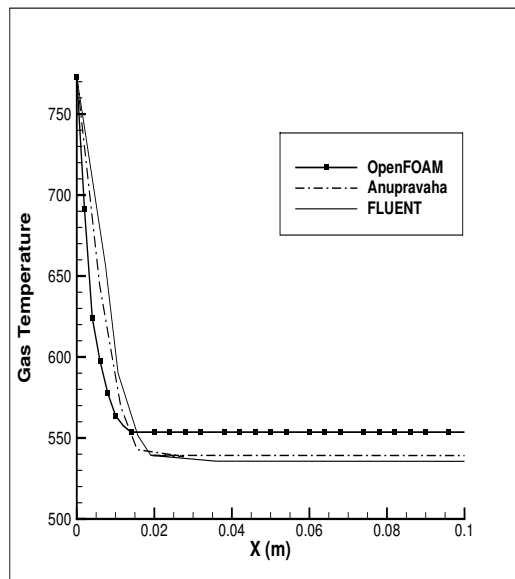


Figure 4.23: Case 4: Variation of Gas Temperature (in K) along the length of the channel

4.5 CASE 5: Gas-Droplet flow with isothermal walls

In this case, both the gas phase and droplet phase enter the channel with a velocity of 1 m/s, when the inlet droplet temperature is equal to the saturation temperature of n-heptane. The inlet properties are given in Table. 4.6. This case differs from the Case 1 by the boundary conditions applied at the walls for gaseous phase temperature. Instead of insulated boundary condition, as in previous cases Dirichlet boundary condition of 1000 K is applied at the both walls. Contour plots are shown in Fig.4.24 to Fig.4.27. From the contour plots, it is observed that evaporation length is shorter compared to Case 1 because of the isothermal boundary condition. Comparison of some parameters along the length of the channel are given in Fig.4.28 and Fig.4.29.

Table 4.6: Case 5: Inlet Conditions

Inlet conditions	
Gas-phase inlet velocity	1.0 <i>m/s</i>
Droplet-phase inlet velocity	1.0 <i>m/s</i>
Inlet gas temperature	773.0 <i>K</i>
Inlet gas temperature	347.8 <i>K</i>
Inlet fuel mass fraction	0.0
Gas-phase inlet density	1.225 <i>kg/m³</i>
Inlet volume fraction	0.0005
Droplet inlet diameter	50 <i>μm</i>

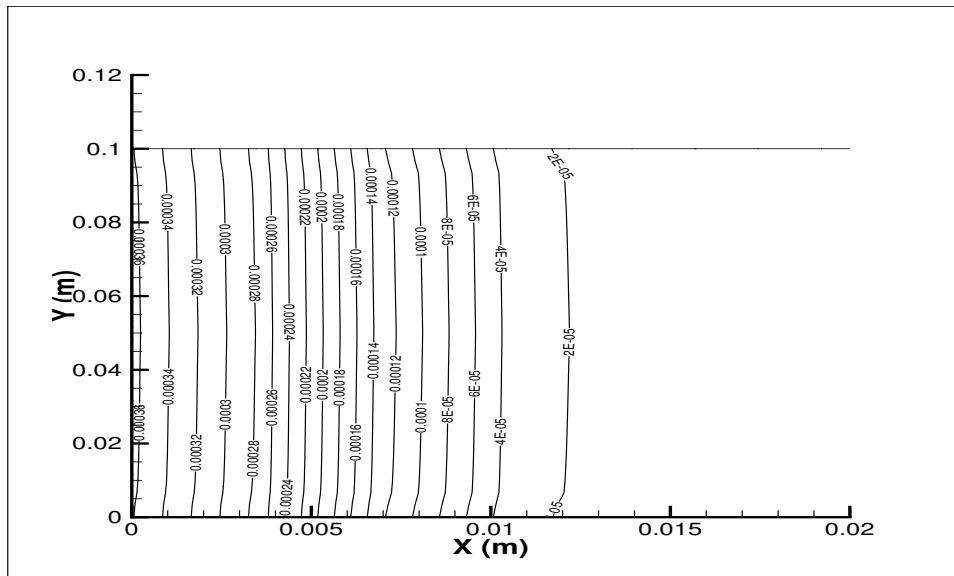


Figure 4.24: Case 5: Contour plot for droplet volume fraction

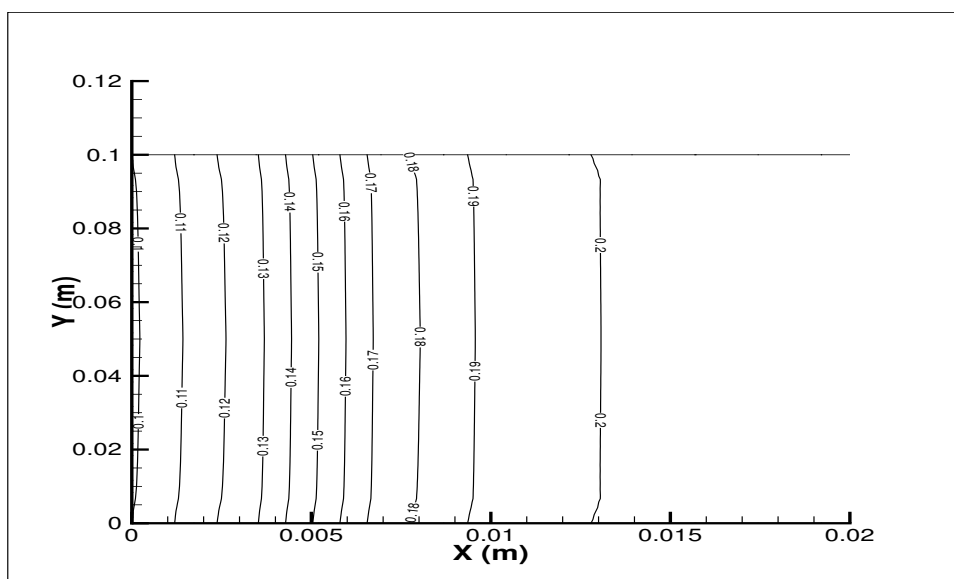


Figure 4.25: Case 5: Contour plot for evaporated fuel mass fraction

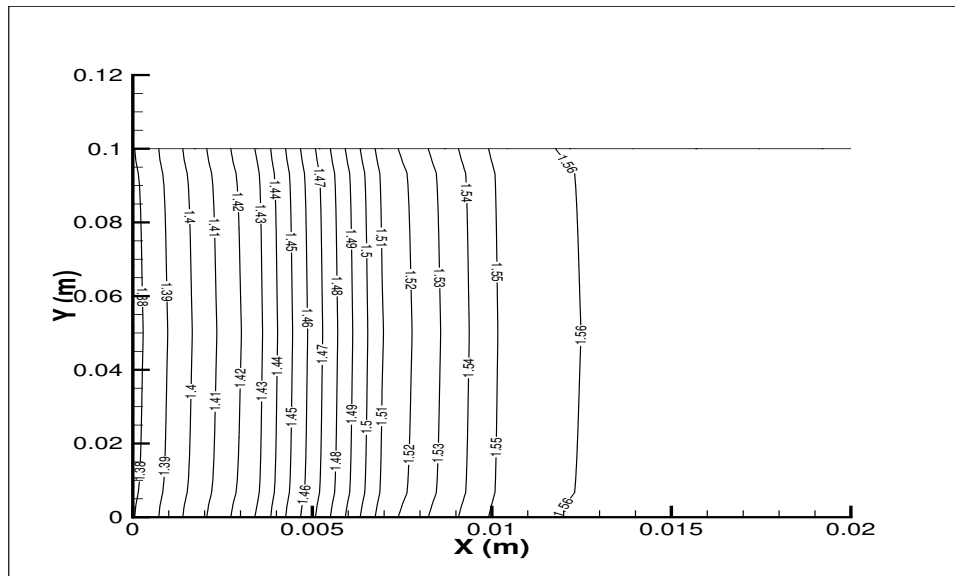
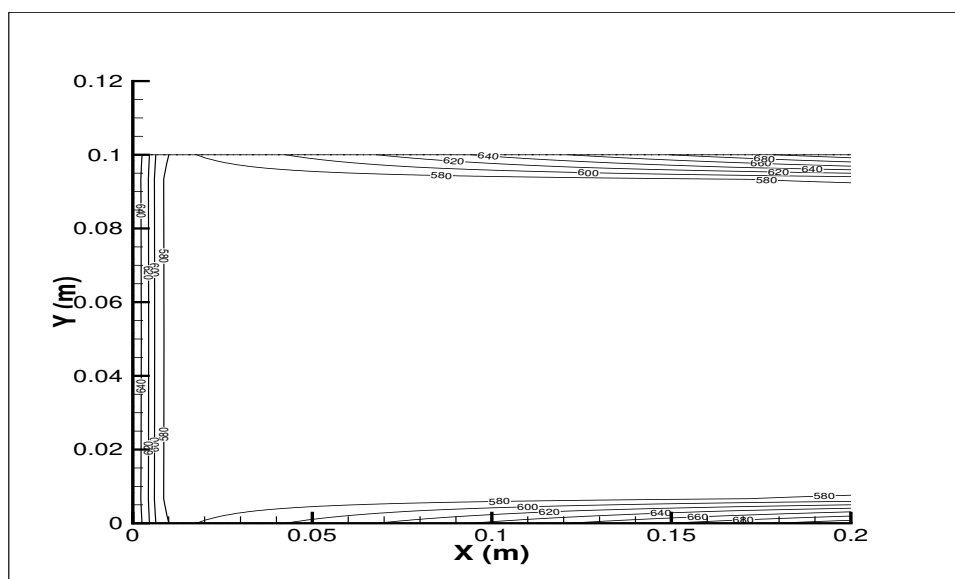
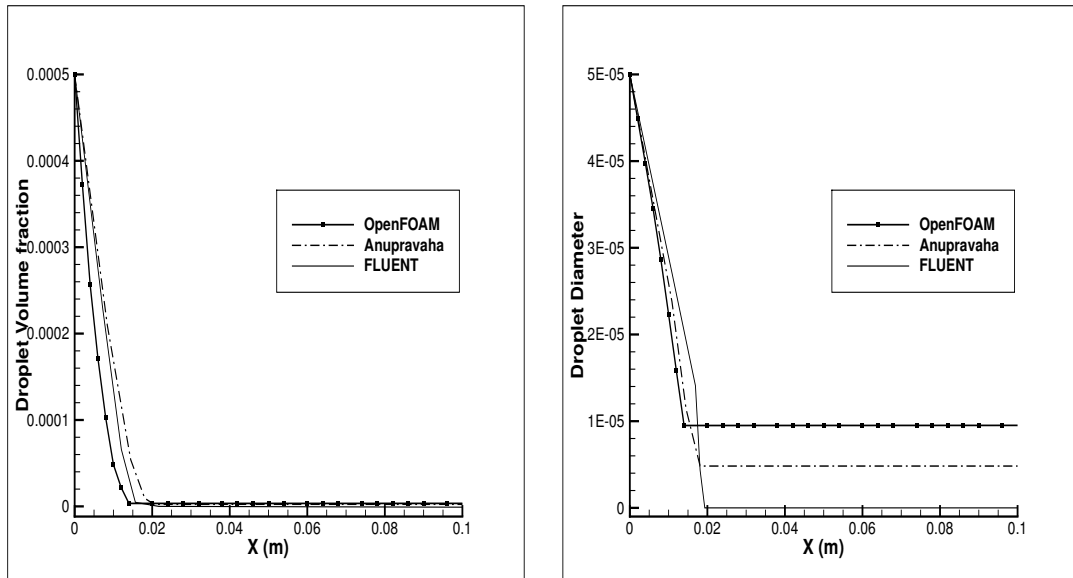
Figure 4.26: Case 5: Contour plot for gas density (in kg/m^3)

Figure 4.27: Case 5: Contour plot for gas temperature (in K)



(a) Case 5: Droplet volume fraction

(b) Case 5: Droplet Diameter (in m)

Figure 4.28: Case 5: Variation along the length of the channel

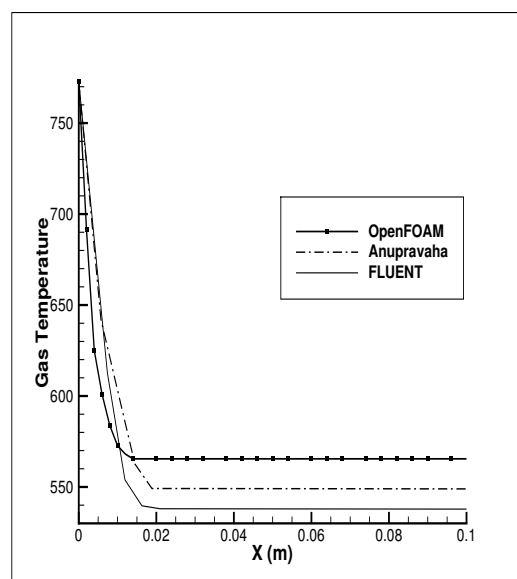


Figure 4.29: Case 5: Variation of Gas Temperature (in K) along the length of the channel

4.6 Closure

The OpenFOAM based solver for ‘dilute laminar gas-droplet flow with evaporation’ has been validated against the Anupravaha solver and FLUENT, with the help of five test problems. It is found to give satisfactory results. This work has allowed for extending the present OpenFOAM multiphase solvers for droplet with evaporation. The initial plan of extending the solver capability for turbulent gas-droplet flow couldn’t get completed. But a proposal for the same has been made in this work along with an evaporation model. This model can be used for further development of the solver. Adding the turbulence model and further validations in it will make this solver more complete.

Chapter 5

Proposal for Dilute Turbulent Gas-Droplet Flows with Evaporation Model

This section deals with the proposal for a mathematical model for dilute turbulent gas-droplet flow with evaporation based on a two-fluid model, which was discussed in Section 1.5. In this model turbulent quantities are modelled with a two-equation ($k - \epsilon$) model.

5.1 Properties of Turbulence

Fluid flows, either single phase flows or two-phase flows, encountered in engineering applications are generally turbulent. Turbulent flows are characterized by

1. Fluid velocity, pressure, other scalar quantities are random and chaotic in nature.
2. Transport: mixing of fluid occurs much more than in laminar due to velocity fluctuations.
3. Generally occurs at high Reynolds numbers.
4. Turbulent flow is characterized by fluctuations over a wide range of length scales and time scales.
5. The fluctuations are always three dimensional even if mean flow field is two dimensional.

6. Energy dissipation due to viscosity is more compared to laminar flow.

5.2 Reynolds Averaging

One important feature of turbulent flow is that velocity, pressure and other scalars at each spatial point vary continuously with time. In most engineering applications, however fluctuating quantities are not of much practical interest. Only the effect of the fluctuating quantities on the mean turbulent motion is needed. So the instantaneous equations needed to be averaged and here we have used Reynolds averaging for droplet phase and Favre averaging, which is explained in section. 5.3 for gaseous phase.

Reynolds averaged equation are obtained by decomposing flow variables into mean or ensemble-averaged and fluctuating component i.e,

$$u_i = U_i + u'_i$$

where, U_i is the mean component and u'_i is fluctuating part of the velocity.

RANS equations are transport equations of mean flow variables. Density fluctuations of droplet phase is assumed to be zero. Substituting the above mentioned relation in all instantaneous (laminar) governing equations given in section.2 and applying the properties of turbulent fluctuating variables i.e.,

$$\overline{u'_i} = 0, \tag{5.1}$$

we will get the averaged equations.

So an ensemble averaged , also called Reynolds averaged governing equations are solved, which introduces new apparent stresses known as Reynolds stresses ($\rho u'_i u'_j$) which comes from the Reynolds averaging of the instantaneous governing equations. These stresses have to be modelled.

5.2.1 Eddy Viscosity Models

Currently, EVMs are most widely used to model the Reynolds stresses because of their relative simplicity and lower computational requirements. In these models, one assumes that the turbulent stress is proportional to the mean rate of strain, this is called the Boussinesq approximation of turbulence. It results in the use a proportionality constant (called turbulent viscosity or eddy viscosity), which

replaces the molecular viscosity in the strain terms. However, unlike molecular viscosity, eddy viscosity is not a property of fluid but it is a property of the motion.

The eddy viscosity is estimated from turbulent transport quantities like turbulent kinetic energy(k), turbulent kinetic energy dissipation(ϵ), specific dissipation rate(ω). These quantities themselves are obtained by solving partial differential transport equations.

The EVMs are often referred to by the number of transport equations, that requires to be solved to estimate the eddy viscosity. For example, the mixing length model is a zero equation model because no transport equations are solved, the Spalart-Almaras is a one equation model as one equation is solved directly for the turbulent viscosity, and the $(k - \epsilon)$ and $(k - \omega)$ models are two equation models because two transport equations are solved, respectively for k and ϵ and for k and ω .

Most EVMs are based on a transport equation for turbulent kinetic energy k which forms the velocity scale, and an additional transport equation for a second turbulent quantity for length/time scale, e.g. dissipation rate of turbulent kinetic energy in the $(k - \epsilon)$, specific dissipation rate of turbulent kinetic energy in the $(k - \omega)$ models, etc.

5.3 Favre Averaging

Taking the density variation of gaseous phase due to mixing of vapour from droplets, density fluctuations should also be considered. Conventional Reynolds averaging(or time-averaging) ignores density fluctuation, and hence is suitable only for incompressible constant-density flows. For variable density flows another averaging method named, Favre Averaging, is used. It's the density-weighted averaging procedure suggested by Favre (1965)[48]. Mass-averaged velocity, u_i is defined by

$$\tilde{u}_i = \frac{1}{\bar{\rho}} \lim_{T \rightarrow +\infty} \int_t^{t+T} \rho(X, \tau) u_i(X, \tau) d\tau \quad (5.2)$$

where, $\bar{\rho}$ is the conventional Reynolds averaged density. Thus, we can say that

$$\bar{\rho} \tilde{u}_i = \bar{\rho} U_i + \overline{\rho' u'_i} \quad (5.3)$$

where an overbar denotes conventional Reynolds average. When we use Favre averaging, as a first step, decompose the instantaneous variable (velocity, temperature) into the mass averaged part (\tilde{u}_i) and a fluctuating part (u_i''),

$$u_i = \tilde{u}_i + u_i'' \quad (5.4)$$

Now, to form the Favre average, we simply multiply through by ρ and do a time average. Hence Eqn.(5.4) becomes

$$\overline{\rho u_i} = \bar{\rho} \tilde{u}_i + \overline{\rho u_i''} \quad (5.5)$$

But, from Eqn.(5.2), we see, Favre average of fluctuating velocity, u_i'' , vanishes, i.e.,

$$\overline{\rho u_i''} = 0 \quad (5.6)$$

But, it is important to note that conventional Reynolds average of u_i'' is not zero. i.e.,

$$\overline{u_i''} \neq 0 \quad (5.7)$$

Favre averaging has simplified the averaging procedure, by eliminating density fluctuations from the averaged equations, but it does not remove the effect of density fluctuations on turbulence. Hence, we can simply say it as a mathematical simplification, not a physical one.

5.4 Assumptions

Apart from the assumptions, which we considered for the laminar flow given in section. 2.1,

1. Third order turbulent fluctuations are neglected.
2. Modification of ϵ -equation due to evaporation is neglected.

5.5 Favre averaged governing equations for the gas phase

In the subsections below, we derive the Favre-averaged turbulent two-phase flow for the two fluid model.

5.5.1 Favre averaged continuity equation

The laminar flow equation is

$$\frac{\partial \vartheta_g \rho_g}{\partial t} + \frac{\partial \vartheta_g \rho_g u_{gj}}{\partial x_j} = n \dot{m}_v$$

$$\vartheta_g \cong 1$$

Convective term of continuity equation is averaged as

$$\overline{\frac{\partial \vartheta_g \rho_g u_{gj}}{\partial x_j}} = \overline{\frac{\partial \vartheta_g \rho_g (\tilde{u}_{gj} + u''_{gj})}{\partial x_j}} = \overline{\frac{\partial \vartheta_g \rho_g \tilde{u}_{gj}}{\partial x_j}} + \overline{\frac{\partial \vartheta_g \rho_g u''_{gj}}{\partial x_j}} = \frac{\partial \vartheta_g \overline{\rho_g} \tilde{u}_{gj}}{\partial x_j}$$

Hence averaged continuity equation becomes

$$\frac{\partial \vartheta_g \overline{\rho_g}}{\partial t} + \frac{\partial \vartheta_g \overline{\rho_g} \tilde{u}_{gj}}{\partial x_j} = n \dot{m}_v \quad (5.8)$$

5.5.2 Favre averaged momentum equation

The laminar equation is

$$\frac{\partial \vartheta_g \rho_g u_{gi}}{\partial t} + \frac{\partial \vartheta_g \rho_g u_{gi} u_{gj}}{\partial x_j} = \vartheta_g \frac{\partial p}{\partial x_i} + \frac{\partial}{\partial x_j} \left[\vartheta_g \mu_g \left(\frac{\partial u_{gi}}{\partial x_j} + \frac{\partial u_{gj}}{\partial x_i} - \frac{2}{3} \frac{\partial u_{gk}}{\partial x_k} \delta_{ij} \right) \right]$$

$$+ \vartheta_g \rho_g g_i - \vartheta_d f_{di} + n \dot{m}_v u_{di} \quad (5.9)$$

substituting $u_g = \tilde{u}_g + u''_g$ and $p = P + p'$ averaging and applying statistical properties of turbulent fluctuating properties, we get averaged equation.

Transient term

$$\overline{\frac{\partial \vartheta_g \rho_g u_{gj}}{\partial t}} = \overline{\frac{\partial \vartheta_g \rho_g (\tilde{u}_{gj} + u''_{gj})}{\partial t}} = \overline{\frac{\partial \vartheta_g \rho_g \tilde{u}_{gj}}{\partial t}} + \overline{\frac{\partial \vartheta_g \rho_g u''_{gj}}{\partial t}} = \frac{\partial \vartheta_g \overline{\rho_g} \tilde{u}_{gj}}{\partial t} \quad (5.10)$$

Convective term

$$\overline{\frac{\partial \vartheta_g \rho_g u_{gi} u_{gj}}{\partial x_j}} = \overline{\frac{\partial \vartheta_g \rho_g (\tilde{u}_{gi} + u''_{gi})(\tilde{u}_{gj} + u''_{gj})}{\partial x_j}} = \overline{\frac{\partial \vartheta_g \rho_g \tilde{u}_{gi} \tilde{u}_{gj}}{\partial x_j}} + \overline{\frac{\partial \vartheta_g \rho_g \tilde{u}_{gi} u''_{gj}}{\partial x_j}}$$

$$+ \overline{\frac{\partial \vartheta_g \rho_g \tilde{u}_{gj} u''_{gi}}{\partial x_j}} + \overline{\frac{\partial \vartheta_g \rho_g u''_{gi} u''_{gj}}{\partial x_j}} \quad (5.11)$$

since $\left(\overline{\frac{\partial \vartheta_g \rho_g \tilde{u}_{gi} u''_{gj}}{\partial x_j}} = 0 = \overline{\frac{\partial \vartheta_g \rho_g \tilde{u}_{gj} u''_{gi}}{\partial x_j}} \right)$

$$\overline{\frac{\partial \vartheta_g \rho_g u_{gi} u_{gj}}{\partial x_j}} = \overline{\frac{\partial \vartheta_g \rho_g \tilde{u}_{gi} \tilde{u}_{gj}}{\partial x_j}} + \overline{\frac{\partial \vartheta_g \rho_g u''_{gi} u''_{gj}}{\partial x_j}} \quad (5.12)$$

Pressure term

$$\overline{-\vartheta_g \frac{\partial p}{\partial x_i}} = \overline{-\vartheta_g \frac{\partial(P + p')}{\partial x_i}} = -\vartheta_g \frac{\partial P}{\partial x_i} + \overline{-\vartheta_g \frac{\partial p'}{\partial x_i}} = -\vartheta_g \frac{\partial P}{\partial x_i} \quad (5.13)$$

Diffusion term

$$\begin{aligned} & \overline{\frac{\partial}{\partial x_j} \left[\vartheta_g \mu_g \left(\frac{\partial u_{gi}}{\partial x_j} + \frac{\partial u_{gj}}{\partial x_i} - \frac{2}{3} \frac{\partial u_{gk}}{\partial x_k} \delta_{ij} \right) \right]} \\ &= \overline{\frac{\partial}{\partial x_j} \left[\vartheta_g \mu_g \left(\frac{\partial(\tilde{u}_{gi} + u''_{gi})}{\partial x_j} + \frac{\partial(\tilde{u}_{gj} + u''_{gj})}{\partial x_i} - \frac{2}{3} \frac{\partial(\tilde{u}_{gk} + u''_{gk})}{\partial x_k} \delta_{ij} \right) \right]} \\ &= \overline{\frac{\partial}{\partial x_j} \left[\vartheta_g \mu_g \left(\frac{\partial \tilde{u}_{gi}}{\partial x_j} + \frac{\partial \tilde{u}_{gj}}{\partial x_i} - \frac{2}{3} \frac{\partial \tilde{u}_{gk}}{\partial x_k} \delta_{ij} \right) \right]} + \overline{\frac{\partial}{\partial x_j} \left[\vartheta_g \mu_g \frac{\partial u''_{gi}}{\partial x_j} \right]} \\ & \quad + \overline{\frac{\partial}{\partial x_j} \left[\vartheta_g \mu_g \frac{\partial u''_{gj}}{\partial x_i} \right]} - \overline{\frac{2}{3} \frac{\partial}{\partial x_j} \left[\vartheta_g \mu_g \frac{\partial u''_{gk}}{\partial x_k} \delta_{ij} \right]} \\ &= \overline{\frac{\partial}{\partial x_j} \left[\vartheta_g \mu_g \left(\frac{\partial \tilde{u}_{gi}}{\partial x_j} + \frac{\partial \tilde{u}_{gj}}{\partial x_i} - \frac{2}{3} \frac{\partial \tilde{u}_{gk}}{\partial x_k} \delta_{ij} \right) \right]} \end{aligned} \quad (5.14)$$

Body force term

$$\overline{\vartheta_g \rho_g g_i} = \vartheta_g \overline{\rho_g} g_i \quad (5.15)$$

Interphase force term (Drag force)

$$\overline{I.F_{di}} = \overline{\vartheta_d f_{di}} \quad (5.16)$$

Evaporation term

$$\overline{n \dot{m}_v u_{di}} = \overline{n \dot{m}_v (\tilde{u}_{di} + u''_{di})} = n \dot{m}_v \tilde{u}_{di} + \overline{n \dot{m}_v u''_{di}} = n \dot{m}_v \tilde{u}_{di} \quad (5.17)$$

Combining all term together, we will get the whole equation as

$$\begin{aligned} \frac{\partial \vartheta_g \overline{\rho_g} \tilde{u}_{gi}}{\partial t} + \frac{\partial \vartheta_g \overline{\rho_g} \tilde{u}_{gi} \tilde{u}_{gj}}{\partial x_j} &= -\vartheta_g \frac{\partial P}{\partial x_i} + \frac{\partial}{\partial x_j} \left[\vartheta_g \mu_g \left(\frac{\partial \tilde{u}_{gi}}{\partial x_j} + \frac{\partial \tilde{u}_{gj}}{\partial x_i} - \frac{2}{3} \frac{\partial \tilde{u}_{gk}}{\partial x_k} \delta_{ij} \right) \right] \\ & \quad - \overline{\vartheta_g \rho_g u''_{gi} u''_{gj}} + \vartheta_g \overline{\rho_g} g_i + \overline{\vartheta_d f_{di}} + n \dot{m}_v \tilde{u}_{di} \end{aligned} \quad (5.18)$$

where $\overline{\rho_g u''_{gi} u''_{gj}}$ (R_{ij}) is the Reynolds stress tensor, having three normal components and six shear stress components. For the closure of problem, modeling of these stresses are required. As R_{ij} is symmetric, number of unknowns are reduced

to six. We can model this using Boussinesq eddy viscosity hypothesis similar to the single phase flows which is given as

$$-\overline{\rho_g u_{gi}'' u_{gj}''} = \mu_{tg} \left[\frac{\partial \tilde{u}_{gi}}{\partial x_j} + \frac{\partial \tilde{u}_{gj}}{\partial x_i} - \frac{2}{3} \frac{\partial \tilde{u}_{gk}}{\partial x_k} \delta_{ij} - \frac{2}{3} \frac{\partial}{\partial x_j} \left(\frac{2}{3} \bar{\rho}_g \tilde{k}_g \delta_{ij} \right) \right] \quad (5.19)$$

substituting this in the above equation, we get modified FANS equation. It is given as

$$\begin{aligned} \frac{\partial \vartheta_g \bar{\rho}_g \tilde{u}_{gi}}{\partial t} + \frac{\partial \vartheta_g \bar{\rho}_g \tilde{u}_{gi} \tilde{u}_{gj}}{\partial x_j} = & -\vartheta_g \frac{\partial P}{\partial x_i} + \frac{\partial}{\partial x_j} \left[\vartheta_g (\mu_g + \mu_{tg}) \left(\frac{\partial \tilde{u}_{gi}}{\partial x_j} + \frac{\partial \tilde{u}_{gj}}{\partial x_i} - \frac{2}{3} \frac{\partial \tilde{u}_{gk}}{\partial x_k} \delta_{ij} \right) \right] \\ & \mu_{tg} \frac{\partial}{\partial x_j} \left(\frac{2}{3} \bar{\rho}_g \tilde{k}_g \delta_{ij} \right) + \vartheta_g \bar{\rho}_g g_i - \overline{\vartheta_d f_{di}} + n \dot{m}_v \tilde{u}_{di} \end{aligned} \quad (5.20)$$

and can be written as,

$$\begin{aligned} \frac{\partial \vartheta_g \bar{\rho}_g \tilde{u}_{gi}}{\partial t} + \frac{\partial \vartheta_g \bar{\rho}_g \tilde{u}_{gi} \tilde{u}_{gj}}{\partial x_j} = & -\vartheta_g \frac{\partial P}{\partial x_i} + \frac{\partial}{\partial x_j} \left[\vartheta_g (\mu_{effg}) \left(\frac{\partial \tilde{u}_{gi}}{\partial x_j} + \frac{\partial \tilde{u}_{gj}}{\partial x_i} - \frac{2}{3} \frac{\partial \tilde{u}_{gk}}{\partial x_k} \delta_{ij} \right) \right] \\ & \mu_{tg} \frac{\partial}{\partial x_j} \left(\frac{2}{3} \bar{\rho}_g \tilde{k}_g \delta_{ij} \right) + \vartheta_g \bar{\rho}_g g_i - \overline{\vartheta_d f_{di}} + n \dot{m}_v \tilde{u}_{di} \end{aligned} \quad (5.21)$$

where $\mu_{effg} = \mu_g + \mu_{tg}$, μ_{tg} is turbulent viscosity and μ_{effg} is the effective viscosity of gaseous phase.

5.5.3 Favre averaged temperature equation

The laminar equation is given as

$$\frac{\partial \vartheta_g \rho_g C_{pg} T_g}{\partial t} + \frac{\partial \vartheta_g \rho_g C_{pg} T_g u_{gj}}{\partial x_j} = \frac{\partial}{\partial x_i} \left(\vartheta_g k_g \frac{\partial T_g}{\partial x_j} \right) + n \dot{m}_v C_{vd} T_d - \dot{Q} \quad (5.22)$$

Applying $T_g = \tilde{T}_g + T_g''$ along with velocity relation, we get

Transient term

$$\overline{\frac{\partial \vartheta_g \rho_g C_{pg} T_g}{\partial t}} = \overline{\frac{\partial \vartheta_g \rho_g C_{pg} (\tilde{T}_g + T_g'')}{\partial t}} = \frac{\partial \vartheta_g \bar{\rho}_g C_{pg} \tilde{T}_g}{\partial t} + \overline{\frac{\partial \vartheta_g \rho_g C_{pg} T_g''}{\partial t}} = \frac{\partial \vartheta_g \bar{\rho}_g C_{pg} \tilde{T}_g}{\partial t}$$

Convective term

$$\begin{aligned} \overline{\frac{\partial \vartheta_g \rho_g C_{pg} T_g u_{gj}}{\partial x_j}} &= \overline{\frac{\partial \vartheta_g \rho_g C_{pg} (\tilde{T}_g + T_g'') (\tilde{u}_{gj} + u_{gj}'')}{\partial x_j}} = \overline{\frac{\partial \vartheta_g \rho_g C_{pg} \tilde{T}_g u_{gj}}{\partial x_j}} + \overline{\frac{\partial \vartheta_g \rho_g C_{pg} \tilde{T}_g u_{gj}''}{\partial x_j}} \\ &\quad + \overline{\frac{\partial \vartheta_g \rho_g C_{pg} T_g' \tilde{u}_{gj}}{\partial x_j}} + \overline{\frac{\partial \vartheta_g \rho_g C_{pg} T_g'' u_{gj}''}{\partial x_j}} \\ &= \overline{\frac{\partial \vartheta_g \rho_g C_{pg} \tilde{T}_g \tilde{u}_{gj}}{\partial x_j}} + \overline{\frac{\partial \vartheta_g \rho_g C_{pg} T_g'' u_{gj}''}{\partial x_j}} \end{aligned}$$

Diffusion term

$$\overline{\frac{\partial}{\partial x_i} \left(\vartheta_g k_g \frac{\partial T_g}{\partial x_j} \right)} = \frac{\partial}{\partial x_i} \left(\vartheta_g k_g \frac{\partial \tilde{T}_g}{\partial x_j} \right) + \overline{\frac{\partial}{\partial x_i} \left(\vartheta_g k_g \frac{\partial T_g''}{\partial x_j} \right)} = \frac{\partial}{\partial x_i} \left(\vartheta_g k_g \frac{\partial \tilde{T}_g}{\partial x_j} \right)$$

Source terms

$$\overline{nm_v C_{vd} T_d} = \overline{nm_v C_{vd} (\tilde{T}_d + T_d'')} = nm_v C_{vd} \tilde{T}_d + \overline{nm_v C_{vd} T_d''} = nm_v C_{vd} \tilde{T}_d$$

Hence averaged temperature equation becomes,

$$\frac{\partial \vartheta_g \rho_g C_{pg} \tilde{T}_g}{\partial t} + \frac{\partial \vartheta_g \rho_g C_{pg} \tilde{T}_g \tilde{u}_{gj}}{\partial x_j} + \overline{\frac{\partial \vartheta_g \rho_g C_{pg} T_g'' u_{gj}''}{\partial x_j}} = \frac{\partial}{\partial x_i} \left(\vartheta_g k_g \frac{\partial \tilde{T}_g}{\partial x_j} \right) + nm_v C_{vd} \tilde{T}_d - n\dot{Q} \quad (5.23)$$

For closure, we have to model the fluctuating term of the temperature equation.

$$\overline{\frac{\partial \vartheta_g \rho_g C_{pg} T_g'' u_{gj}''}{\partial x_j}} = \overline{\frac{\partial \vartheta_g \rho_g C_{pg} T_g'' u_{gj}''}{\partial x_j}}$$

As we assume derivatives do not fluctuate,

$$\overline{T_g'' u_{gj}''} = -\alpha_{tg} \frac{\partial \tilde{T}_g}{\partial x_j}$$

where α_{tg} is the turbulent diffusivity, s.t. $\alpha_{tg} \equiv \frac{k_{tg}}{\rho C_p}$. Usually α_t is equal to $\frac{\nu_{tg}}{Pr_{tg}}$, where ν_{tg} is turbulent kinematic viscosity of gaseous phase and Pr_{tg} is turbulent Prandtl number of gaseous phase. Usually value of Pr_{tg} is taken as 0.9. Substituting this in the temperature equation we get the closed equation. It is given as

$$\frac{\partial \vartheta_g \rho_g C_{pg} \tilde{T}_g}{\partial t} + \frac{\partial \vartheta_g \rho_g C_{pg} \tilde{T}_g \tilde{u}_{gj}}{\partial x_j} = \frac{\partial}{\partial x_i} \left(\vartheta_g (k_g + k_{tg}) \frac{\partial \tilde{T}_g}{\partial x_j} \right) + nm_v C_{vd} \tilde{T}_d - n\dot{Q} \quad (5.24)$$

5.5.4 Favre Averaged Species Mass Fraction Equation

The laminar equation is given as

$$\frac{\partial(\vartheta_g \rho_g Y_F)}{\partial t} + \frac{\partial(\vartheta_g \rho_g Y_F u_{gj})}{\partial x_j} = \frac{\partial}{\partial x_i} (\vartheta_g \rho_g D \frac{\partial Y_F}{\partial x_j}) + n \dot{m}_v \quad (5.25)$$

Similar, to the temperature equation, we can deduce averaged equation. Only difference is that instead of temperature another scalar, fuel vapour mass fraction is the variable. The averaging yields the equation in the following form,

$$\frac{\partial(\vartheta_g \bar{\rho}_g \tilde{Y}_F)}{\partial t} + \frac{\partial(\vartheta_g \bar{\rho}_g \tilde{Y}_F \tilde{u}_{gj})}{\partial x_j} + \frac{\partial(\overline{\vartheta_g \rho_g Y_F'' u_{gj}''})}{\partial x_j} = \frac{\partial}{\partial x_i} (\vartheta_g \bar{\rho}_g D \frac{\partial \tilde{Y}_F}{\partial x_j}) + n \dot{m}_v \quad (5.26)$$

such that,

$$\overline{\vartheta_g Y_F'' u_{gj}''} = -D_\tau \frac{\partial \tilde{Y}_F}{\partial x_j}, \quad \text{where } D_\tau = \frac{\mu_{tg}}{Sc_{tg}}$$

where, Sc_{tg} is the turbulent Schmidt number of gaseous phase. Its value is taken as 0.9. Hence the final form of the averaged equation is

$$\frac{\partial(\vartheta_g \bar{\rho}_g \tilde{Y}_F)}{\partial t} + \frac{\partial(\vartheta_g \bar{\rho}_g \tilde{Y}_F \tilde{u}_{gj})}{\partial x_j} = \frac{\partial}{\partial x_i} (\vartheta_g \bar{\rho}_g (D + D_\tau) \frac{\partial \tilde{Y}_F}{\partial x_j}) + n \dot{m}_v \quad (5.27)$$

5.6 Reynolds Averaged Equations for the Droplet Phase

The Reynolds averaging method is developed here in the droplet phase. Flow variables are divided into mean and fluctuating part as we discussed in section.5.2 and closure procedure is conducted.

By Substituting the following expressions:

$$u_d = U_d + u'_d$$

$$\vartheta_d = V_d + \vartheta'_d$$

$$T_d = \bar{T}_d + T'_d$$

and performing averaging, we get the Reynolds averaged equations for droplet phase as the following.

5.6.1 Reynolds Averaged Continuity Equation

The laminar equation is

$$\frac{\partial \rho_d \vartheta_d}{\partial t} + \frac{\partial \rho_d \vartheta_d u_{d,j}}{\partial x_j} = -n\dot{m}_v \quad (5.28)$$

Transient term

$$\overline{\frac{\partial \rho_d \vartheta_d}{\partial t}} = \overline{\frac{\partial \rho_d (V_d + \vartheta'_d)}{\partial t}} = \frac{\partial V_d \rho_d}{\partial t} + \overline{\frac{\partial \vartheta'_d \rho_d}{\partial t}} = \frac{\partial V_d \rho_d}{\partial t}$$

Convective Term

$$\begin{aligned} \overline{\frac{\partial \rho_d \vartheta_d U_{d,j}}{\partial x_j}} &= \overline{\frac{\partial (V_d + \vartheta'_d) \rho_d (U_{d,j} + u'_{d,j})}{\partial x_j}} = \frac{\partial V_d \rho_d U_{d,j}}{\partial x_j} + \overline{\frac{\partial \vartheta'_d \rho_d U_{d,j}}{\partial x_j}} + \overline{\frac{\partial V_d \rho_d u'_{d,j}}{\partial x_j}} + \overline{\frac{\partial \vartheta'_d \rho_d u'_{d,j}}{\partial x_j}} \\ &= \frac{\partial V_d \rho_d U_{d,j}}{\partial x_j} + \overline{\frac{\partial \rho_d \vartheta'_d u'_{d,j}}{\partial x_j}} \end{aligned}$$

Substituting these in continuity equation, we get

$$\frac{\partial \rho_d V_d}{\partial t} + \frac{\partial \rho_d V_d U_{d,j}}{\partial x_j} + \overline{\frac{\partial \vartheta'_d \rho_d u'_{d,j}}{\partial x_j}} = -n\dot{m}_v \quad (5.29)$$

As, $\overline{\vartheta'_d u'_{d,j}} = -D_d \frac{\partial V_d}{\partial x_j}$ and $D_{td} = \frac{\nu_{td}}{Pr_{td}}$ where, D_{td} is the turbulent mass dispersity of the droplets. We get the final equation as,

$$\frac{\partial \rho_d V_d}{\partial t} + \frac{\partial \rho_d V_d U_{d,j}}{\partial x_j} = \frac{\partial \rho_d (D_d \frac{\partial V_d}{\partial x_j})}{\partial x_j} - n\dot{m}_v \quad (5.30)$$

where, ν_{td} is the turbulent kinematic viscosity of droplet phase and Pr_{td} is the turbulent dispersion Prandtl number.

5.6.2 Reynolds Averaged momentum equation

The laminar equation is given as

$$\frac{\partial (\vartheta_d \rho_d u_{d,i})}{\partial t} + \frac{\partial (\vartheta_d \rho_d u_{d,i} u_{d,j})}{\partial x_j} = -\vartheta_d \frac{\partial P}{\partial x_i} + \vartheta_d \rho_d \mathbf{g}_i - n\dot{m}_v u_{d,i} + \vartheta_d \mathbf{f}_{d,i} \quad (5.31)$$

Transient term

$$\begin{aligned} \overline{\frac{\partial (\vartheta_d \rho_d u_{d,i})}{\partial t}} &= \overline{\frac{\partial (V_d + \vartheta'_d) \rho_d (U_{d,i} + u'_{d,i})}{\partial t}} = \frac{\partial V_d \rho_d U_{d,i}}{\partial t} + \overline{\frac{\partial \vartheta'_d \rho_d U_{d,i}}{\partial t}} + \overline{\frac{\partial V_d \rho_d u'_{d,i}}{\partial t}} + \overline{\frac{\partial \vartheta'_d \rho_d u'_{d,i}}{\partial t}} \\ &= \frac{\partial V_d \rho_d U_{d,i}}{\partial t} + \overline{\frac{\partial \rho_d \vartheta'_d u'_{d,i}}{\partial t}} \end{aligned}$$

Convective term

$$\begin{aligned} \overline{\frac{\partial(\vartheta_d \rho_d u_{d,i} u_{d,j})}{\partial x_j}} &= \overline{\frac{\partial(V_d + \vartheta'_d) \rho_d (U_{d,i} + u'_{d,i})(U_{d,j} + u'_{d,j})}{\partial x_j}} = \frac{\partial V_d \rho_d U_{d,i} U_{d,j}}{\partial x_j} + \frac{\partial V_d \rho_d \overline{u'_{d,i} u'_{d,j}}}{\partial x_j} \\ &\quad + \frac{\partial \rho_d U_{d,i} \overline{\vartheta'_d u'_{d,j}}}{\partial x_j} + \frac{\partial \rho_d U_{d,j} \overline{\vartheta'_d u'_{d,i}}}{\partial x_j} + \frac{\partial \rho_d \overline{\vartheta'_d u'_{d,i}}}{\partial x_j} \\ &= \frac{\partial V_d \rho_d U_{d,i} U_{d,j}}{\partial x_j} + \frac{\partial V_d \rho_d \overline{u'_{d,i} u'_{d,j}}}{\partial x_j} + \frac{\partial \rho_d U_{d,i} \overline{\vartheta'_d u'_{d,j}}}{\partial x_j} + \frac{\partial \rho_d U_{d,j} \overline{\vartheta'_d u'_{d,i}}}{\partial x_j} \end{aligned}$$

Pressure term

$$\overline{\vartheta_d \frac{\partial P}{\partial x_i}} = \overline{(V_d + \vartheta'_d) \frac{\partial(P + p')}{\partial x_i}} = V_d \frac{\partial P}{\partial x_i} + \overline{\vartheta'_d \frac{\partial p'}{\partial x_i}} = V_d \frac{\partial P}{\partial x_i}$$

Body force term

$$\overline{\vartheta_d \rho_d \mathbf{g}_i} = \overline{(V_d + \vartheta'_d) \rho_d \mathbf{g}_i} = V_d \rho_d \mathbf{g}_i + \overline{\vartheta'_d \rho_d \mathbf{g}_i} = V_d \rho_d \mathbf{g}_i$$

Substituting all these in momentum equation and neglecting terms involving $\vartheta'_d u'_{d,j}$, we will get averaged equation as

$$\frac{\partial(V_d \rho_d U_{d,i})}{\partial t} + \frac{\partial(V_d \rho_d U_{d,i} U_{d,j})}{\partial x_j} + \frac{\partial V_d \rho_d \overline{u'_{d,i} u'_{d,j}}}{\partial x_j} + \frac{\partial \rho_d U_{d,i} \overline{\vartheta'_d u'_{d,j}}}{\partial x_j} \quad (5.32)$$

$$= -V_d \frac{\partial P}{\partial x_i} + V_d \rho_d \mathbf{g}_i + \overline{\vartheta'_d \mathbf{f}_{d,i}} - n \dot{m}_v U_{d,i} \quad (5.33)$$

$\overline{\rho_d u'_{d,i} u'_{d,j}}$ is modelled as mentioned below

$$\overline{\rho_d u'_{d,i} u'_{d,j}} = \mu_d \left(\frac{\partial U_{d,i}}{\partial x_j} + \frac{\partial U_{d,j}}{\partial x_i} - \frac{2}{3} \frac{\partial U_{d,k}}{\partial x_k} \delta_{ij} \right) - \frac{2}{3} \rho_d k_d \delta_{ij}$$

μ_{td} is the turbulent viscoisty of droplet phase.

$$\nu_{td} = \frac{\mu_{td}}{\rho_d} = K_d \nu_{tg}$$

where, K_d is the weight factor accounting for the particle inertia which is given by

$$K_d = \max \left(K_D, \frac{1}{1 + St_t} \right)$$

Details can be found in Tu. et al,[44].

where, K_D is the numerical dissipation and St_t is the turbulent stokes number and is given by

$$St_t = \frac{t_d}{t_e}$$

where, t_d is the droplet response time which is given as

$$t_d = \frac{\rho_d \vartheta_d d_d * d_d}{18\mu_g}$$

t_e is the eddy characteristic time which is given as

$$t_e = 0.125 \frac{\tilde{k}_g}{\tilde{\epsilon}_g}$$

5.6.3 Reynolds Averaged Temperature Equation

The laminar equation is given as

$$\frac{\partial [\rho_d \vartheta_d C_{ld} T_d]}{\partial t} + \nabla \cdot (\rho_d \vartheta_d C_{ld} T_d \mathbf{u}_d) = -n \dot{m}_v C_{ld} T_d - n \dot{m}_v L + n Q \quad (5.34)$$

Following the same procedure, which has done for the scalar droplet volume fraction equation(i.e., droplet phase continuity equation), we will get the final averaged equation as

$$\frac{\partial \vartheta_d \rho_d C_{ld} \bar{T}_d}{\partial t} + \frac{\partial \vartheta_d \rho_d C_{ld} \bar{T}_d U_{dj}}{\partial x_j} = \frac{\partial}{\partial x_i} \left(\vartheta_d k_{td} \frac{\partial \bar{T}_d}{\partial x_j} \right) - n \dot{m}_v C_{vd} \bar{T}_d - n \dot{m}_v L + n \dot{Q} \quad (5.35)$$

5.7 $k-\epsilon$ Equation of Gaseous Phase

The familiar single phase $k-\epsilon$ equations will get modified due to the presence of droplets. Single phase equations can be found in Wilcox [23]. Mathematically, apart from the additional terms due to evaporation and interfacial force(drag), there will not be any difference between these single phase and two-phase flows. The equations are,

k - Equation

$$\begin{aligned} \frac{\partial \bar{\rho}_g \tilde{k}_g}{\partial t} + \frac{\partial \bar{\rho}_g \tilde{k}_g \tilde{u}_{gj}}{\partial x_j} &= \mu_{tg} \left[\frac{\partial \tilde{u}_{gi}}{\partial x_j} + \frac{\partial \tilde{u}_{gj}}{\partial x_i} - \frac{2}{3} \frac{\partial \tilde{u}_{gk}}{\partial x_k} \delta_{ij} \right] \frac{\partial \tilde{u}_{gi}}{\partial x_j} \\ &+ \frac{\partial}{\partial x_j} \left[\nu_g \left(\mu_g \frac{\partial \tilde{k}_g}{\partial x_j} + \frac{\mu_{tg}}{\bar{\rho}_g \sigma_k} \frac{\partial \bar{\rho}_g \tilde{k}_g}{\partial x_j} \right) \right] - \bar{\rho}_g \tilde{\epsilon}_g + I_k \end{aligned} \quad (5.36)$$

and

ϵ - Equation

$$\begin{aligned} \frac{\partial \bar{\rho}_g \tilde{\epsilon}_g}{\partial t} + \frac{\partial \bar{\rho}_g \tilde{\epsilon}_g \tilde{u}_{gj}}{\partial x_j} &= C_{\epsilon 1} \frac{\tilde{\epsilon}_g}{\tilde{k}_g} \mu_{tg} \left[\frac{\partial \tilde{u}_{gi}}{\partial x_j} + \frac{\partial \tilde{u}_{gj}}{\partial x_i} - \frac{2}{3} \frac{\partial \tilde{u}_{gk}}{\partial x_k} \delta_{ij} \right] \frac{\partial \tilde{u}_{gi}}{\partial x_j} \\ &+ \frac{\partial}{\partial x_j} \left[\nu_g \left(\mu_g \frac{\partial \tilde{\epsilon}_g}{\partial x_j} + \frac{\mu_{tg}}{\bar{\rho}_g \sigma_k} \frac{\partial \bar{\rho}_g \tilde{\epsilon}_g}{\partial x_j} \right) \right] - C_{\epsilon 2} \bar{\rho}_g \frac{\tilde{\epsilon}_g^2}{\tilde{k}_g} + I_\epsilon \end{aligned} \quad (5.37)$$

where, I_k and I_ϵ are the additional terms due to the presence of droplets in k and ϵ equations respectively, which can be written as,

$$I_k = I_{dk} + I_{ek} \quad (5.38)$$

$$I_\epsilon = I_{d\epsilon} + I_{e\epsilon} \quad (5.39)$$

where, suffix 'd' stands for drag force term and suffix 'e' stands for evaporation term.

The drag term in k and ϵ equations are deduced as explained in Chen and Wood[42]. Term due to evaporation is also derived in the same way.

$$I_{dk} = 2 * \bar{\rho}_g * \rho_d * V_d * \frac{\tilde{k}_g}{t_d} * (1 - e^{-0.0825 * \frac{t_d}{t_e}})$$

$$I_{ek} = 2 * \bar{\rho}_g * n * \dot{m}_v * \tilde{k}_g * (e^{-0.0825 * \frac{t_d}{t_e}})$$

I_ϵ is considered to have effects only due to drag. Effects due to evaporation is neglected. It is given as

$$I_\epsilon = I_{d\epsilon} = -2 * \bar{\rho}_g * \rho_d * V_d * \frac{\tilde{\epsilon}_g}{t_d}$$

Then the turbulent kinematic viscosity of gaseous phase is computed using

$$\nu_{tg} = \frac{C_\mu \tilde{k}_g * \tilde{k}_g}{\tilde{\epsilon}_g}$$

Model constants are given as $C_{\epsilon 1} = 1.44$, $C_{\epsilon 2} = 1.92$, $C_{\mu} = 0.09$, $\sigma_{\epsilon} = 1.0$, $\sigma_k = 1.3$, following the practice of single phase flows.

μ_{td} is obtained using value of ν_{tg} as mentioned earlier.

5.8 Solution Algorithm

1. Initialize values of properties and flow variables for both phases, grids and other parameters.
2. Transfer $(n + 1)th$ time level values to nth time level including all solvable variables like volume fraction, velocity, density, temperature for the gas phase and droplet phase, fuel mass fraction and pressure.
3. Compute \dot{m}_v using equation

$$Sh = \frac{\dot{m}_v}{\pi D \rho_g B_M d_d}$$

where Sh is Sherwood number, B_M is mass transfer number, D is the diffusion coefficient.

$$Sh_f(1 + B_{M,f})^{0.7} = 2 + 0.914 Re_M^{1/2} Sc_f^{1/3} (1 + 1.235 I_{\infty}^{0.372})$$

$$Re_M = \frac{\rho_{\infty} d_d U_{\infty}}{\mu_f}$$

$$Sc_f = \frac{\mu_f}{\rho_f D}$$

the suffix f stands for film, ∞ stands for the free stream.

Equation can be found in the work done by Al-Sood[28].

$$I_{\infty} = \frac{u'}{U} = \frac{\sqrt{2k_g/3}}{U} \quad \text{where, } U = \sqrt{u^2 + v^2 + w^2}$$

4. Solve for all other source terms with previous time step values. Compute and store diameter using the following relation

$$d_d = d_o \left(\frac{\vartheta_d}{\vartheta_o} \right)^{\frac{1}{3}}$$

where, d_d and ϑ_o are the initial diameter and volume fraction.

5. Solve Reynolds Averaged Momentum Equation for gaseous phase with the help of previous time step values of k_g and ϵ_g . It's a two-step procedure (predictor-corrector). Along with update the values of k_g and ϵ_g by solving both turbulent transport equations. Here both RANS and turbulent transport equations are coupled. Using the updated values of k_g and ϵ_g , each time update the value of evaporation rate as well.
6. Undertake the same procedure for Averaged Momentum Equation of droplet phase. Here difference from that of gaseous phase is using an empirical relation for finding out the value of kinematic viscosity which depends on k_g and ϵ_g instead of solving droplet phase turbulent transport equation. Each time take values of k_g and ϵ_g and solve for droplet velocity.
7. Repeat the step 5 and 6 together until the global convergence is reached. We now have U_g^{n+1} and U_d^{n+1} .
8. Solve continuity equation of droplet phase to get the mean value of droplet phase to get the mean value of droplet volume fraction. Using it we will get the volume fraction of gaseous phase.

$$\vartheta_g = 1 - \vartheta_d$$

9. Solve then the continuity equation of gaseous phase which help us to get the value of ρ_g^{n+1} .
10. Solve the energy equation for the droplet phase equation for droplet temperature T_d^{n+1} .
11. Solve the evaporated fuel vapour mass fraction equation to obtain Y_F^{n+1} .
12. Solve the gas-phase energy equation to obtain T_g^{n+1} .
13. If the stopping criterion for the time stepping is not met return to step 2 and repeat steps 2 through 12 for the next time step and march forward in time.

Chapter 6

Conclusion and Scope of the Future work

Conclusion

An Eulerian-Eulerian Two-Fluid model for simulating laminar gas-droplet flows has been successfully implemented in an open source CFD solver, *OpenFOAM*. The classical model for droplet evaporation as developed by Splading [10] has been implemented in the module and it was found to give satisfactory results for low and moderate evaporation rates with simplifying assumptions. The evaporation model was tested by solving different test problems and the results obtained were compared with that of obtained by Anupravaha, which was validated by Mrunalini[4]. Results showed a good match between the model predictions and Anupravaha results when compared to the commercial software FLUENT.

Some discrepancies were found in the values of gas-phase density. This is due to the fact that Fluent uses a mixing rule to compute mixture density, while a transport equation for density is solved in the present solver. Fluent keeps the initial diameter value for the calculation of drag force whereas we update the diameter value (using updated droplet volume fraction value), which also cause some discrepancies.

Scope of the Future work

The module is implemented in a general purpose CFD solver for both 2-D and 3-D problems but has been tested only for 2-D problems. The implementation has to be further verified against 3-D test cases. Most of the engineering or practical

applications, as we see are of turbulent in nature. Hence modeling turbulent gas-droplet flow is required, for which a model is proposed in this thesis. It needs to be implemented in the solver. It can be implemented in Anupravaha. The turbulent model would open a way for the solver to simulate problems involving droplet combustion, if combustion modelling is also incorporated in the equations.

The present evaporation model assumes uniform temperature within the droplet which may prove inaccurate for high evaporation rate conditions. Sophisticated evaporation models which take into account the non-equilibrium effects and are suitable for high evaporation rate conditions can also be implemented. These models are able to simulate complex problems like turbulent evaporating sprays involving high droplet Reynolds number and evaporation rate. Detailed analysis and comparison of such models are found in Faeth [13], Miller [32] and Sirignano [2]. Non-uniformity of the droplet temperature can be modeled by adding extra heat transfer terms in the droplet phase energy equation, as done by Miller [32]. Convergence difficulties were observed for gas-droplet flows with very small values of volume fraction ($\leq 5 \times 10^{-6}$) in the domain. Further investigation is needed in this regard.

The solver considers mono-sized, single component droplets. For problems of practical importance continuous size distribution can be represented by droplets with different sizes which correspond to classes of droplets, which each class having its separate set of equations as done by Guo [7]. Many practical applications involving blended fuels require simulation of multi-component droplets. Further development is required in these fields. We have developed a model by neglecting some complex phenomena like droplet break-up, droplet coalescence, internal circulation inside droplet, which can provide inaccuracy especially in dense turbulent flow. The solver can be further developed in this direction.

Appendix A

Properties of fluids used

Our laminar evaporation model is validated using **air** as continuous phase and **n-heptane** as liquid droplet phase. Properties of these fluids are:

A.1 Properties of n-heptane

- Normal boiling Temperature $T_{bn} = 371.6 \text{ K}$, Molecular weight $M_F = 100.204$, Critical temperature $T_{cri} = 540.17 \text{ K}$, Critical pressure $P_{cri} = 2631.633 \text{ kPa}$
- Vapour pressure is obtained by the Clausius-Clapeyron equation as

$$P_{Fs} = \exp\left(14.2146 - \frac{3151.68}{T_d - 43}\right) \text{ for } T_d > T_{bn} \text{ (kPa)} \quad (\text{A.1})$$

$$P_{Fs} = \exp\left(14.3896 - \frac{3209.45}{T_d - 43}\right) \text{ for } T_d \leq T_{bn} \text{ (kPa)} \quad (\text{A.2})$$

where T_d is the droplet temperature in K and T_{bn} is the saturation temperature at atmospheric pressure.

- Latent heat of vaporization as a function of droplet temperature is

$$L = 317.8 \times 1000.0 \left(\frac{540.17 - T_d}{540.17 - 371.4}\right)^{-0.38} \text{ (J/kg)} \quad (\text{A.3})$$

- Specific heat at constant pressure for fuel vapour

$$C_{vd} = (363 + 0.467 T_r) \times (5 - 0.001 \times 883.05) \text{ (J/kg K)} \quad (\text{A.4})$$

- Thermal conductivity of vapour in ($W/m K$)

$$k_v = 10^{-7} \times (14.52 T_{ref} - 5.14)^{2/3} \times (C_{vd} M_F / \lambda) \quad (A.5)$$

where

$$\lambda = T_{cri}^{1/6} \times M_F^{0.5} \left(\frac{P_{atm}}{P_{cri}} \right)^{2/3} \quad (A.6)$$

where $T_{ref} = T_r / T_{cri}$

- Density of liquid fuel, ρ_d in (kg/m^3)

For $T_d \leq 538.0$

$$\rho_d = -941.03 + 19.96181 T_d - 0.08612051 T_d^2 + 1.579494 \times 10^{-4} T_d^3 - 1.089345 \times 10^{-7} T_d^4 \quad (A.7)$$

Otherwise

$$\rho_d = 4.19528 \times 10^7 - 2.360524 \times 10^5 T_d + 442.7316 T_d^2 - 0.2767921 T_d \quad (A.8)$$

where T_r is the reference temperature obtained by the '1/3' rule.

A.2 Properties of Air

- Specific heat at constant pressure for air

$$C_{pa} = c1 + c2 \left(\frac{c3/T_r}{\sinh(c3/T_r)} \right)^2 + c4 \left(\frac{c5/T_r}{\cosh(c5/T_r)} \right)^2 \quad (A.9)$$

where $c1 = 0.2896 \times 10^5$, $c2 = 0.09390 \times 10^5$, $c3 = 3.0120 \times 10^3$, $c4 = 0.0758 \times 10^5$, $c5 = 1484$

In the above expression C_{pa} is in $J/kmol K$

- Thermal conductivity for air in ($W/m K$)

$$k_a = 1.5207 \times 10^{-11} T_r^3 - 4.8574 \times 10^{-8} T_r^2 + 1.0184 \times 10^{-4} T_r - 3.9333 \times 10^{-4} \quad (A.10)$$

References

- [1] ISHII, M. AND HIBIKI, T., “Thermo-Fluid Dynamics of Two-Phase Flow”, *Springer Science+Business Media, Inc.*, 1990.
- [2] SIRIGNANO, W.A., “Fluid dynamics and Transport of Droplets and Sprays”, *Cambridge University Press*, 1999.
- [3] CROWE, C.T., SOMMERFELD, M. AND TSUJI, Y., “Multiphase flows with droplets and particles”, *CRC Press: Boca Raton*, 1998.
- [4] MRUNALINI B., Development of Finite Volume Solver for Dilute Gas-Droplet Flow with Evaporation, Thesis for the Degree of Master of Technology, *Department of Mechanical Engineering*, Indian Institute of Technology Hyderabad, 2012.
- [5] DARWISH, M., MOUKALLED, F. AND SEKAR, B., “A unified formulation of the segregated class of algorithms for multifluid flow at all speeds”, *Numerical Heat Transfer, Part B: Fundamentals*, Vol. 40:2, pp. 99-137, 2001.
- [6] HALLMANN, M., SCHEURLEN, M. AND WITTIG, S., “Computation of turbulent evaporating sprays: Eulerian versus Lagrangian approach”, *J. of Engg. for Gas Turbines and Power, Transactions of ASME*, Vol. 117, pp. 112-119, 1995.
- [7] GUO, Y.C., CHAN, C.K., AND LAU, K.S., “A pure Eulerian model for simulating dilute spray combustion”, *Fuel*, Vol. 81, pp. 2131-2144, 2002.
- [8] FUCHS, N.A., “Evaporation and droplet growth in gaseous media”, *London: Pergamon Press*, 1959.

- [9] GODSAVE, G.A.E., "Studies of the Combustion of Drops in a Fuel Spray-the Burning of Single Drops of Fuel", *Fourth Symposium (International) on the Combustion, Williams and Wilkins, Baltimore*, pp. 818-830, 1953.
- [10] SPALDING, D.B., "The combustion of liquid fuels", *Fourth Symposium (International) on the Combustion, Williams and Wilkins, Baltimore*, pp. 847-864, 1953.
- [11] FROSSLING, N., "On the Evaporation of Falling Droplets", *Gerlands Beitr. Geophys.*, Vol. 52, pp. 170-216, 1938.
- [12] RANZ, W.E., AND MARSHALL, W. R., "Evaporation from Drops", *Chem. Eng. Prog.*, Vol. 48, Part I, pp. 141-146, Part II, pp. 173-180, 1952.
- [13] FAETH, G.M., "Current Status of Droplet and Liquid Combustion", *Prog. Energy Combust. Sci.*, Vol. 3, pp. 191-224, 1977.
- [14] LEFEBVRE, A.H., "Atomization and sprays", *Taylor and Francis*, 1989.
- [15] KENT, J.C., "Quasi-steady diffusion-controlled droplet evaporation and condensation", *Appl. Sci. Res.*, Vol. 28, pp. 315-360, 1973.
- [16] SAZHIN, S.S., "Advanced models of fuel droplet heating and evaporation", *Prog. in Energy and Combustion Sci.*, Vol. 32, pp. 162-214, 2006.
- [17] ABRAMZON, B., AND SIRIGNANO, W.A., "Droplet vaporization model for spray combustion calculation", *Int. J. of Heat and Mass Transfer*, Vol. 32, pp. 1605-1618, 1989.
- [18] PERRY, R H., GREEN, D.W., "Perry's chemical engineers' handbook", *Mc Graw Hill Publications*, 1997.
- [19] REID, R.C., PRAUSNITZ, J.M. AND POLING, B.E., "The properties of gases and liquids", *McGraw-Hill International Editions*, 1988.
- [20] HUBBARD, G.L., DENNY, V. E. AND MILLS, A.F., *Int. J. Heat Mass Transfer*, Vol. 16, pp. 1003-1008, 1973.

- [21] KODELA CHANDRASEKHAR, Numerical Simulation of Turbulent Two-Phase Flows, Thesis for the Degree of Master of Technology, *Department of Mechanical Engineering*, Indian Institute of Technology Kanpur, 2009.
- [22] POPE, S. B., “Turbulent Flows”, *Cambridge University Press*, 2000.
- [23] WILCOX, DAVID C., “Turbulence Modeling for CFD”, *D C W Industries*, 1998-07.
- [24] OLIVER, TODD A., “Favre-averaged Navier–Stokes and turbulence model equation documentation”, *Technical report, Predictive Engineering and Computational Sciences, University of Texas at Austin*, 2011.
- [25] MASHAYEK, F. AND PANDYA, R. V. R., “Analytical description of particle/droplet-laden turbulent flows”, *Progress in Energy and Combustion Sciences*, Vol. 4, pp. 329-378, 2003.
- [26] SLATER, S. A. AND LEEMING, A. D. AND YOUNG, J. B., “Particle deposition from two-dimensional turbulent gas flows”, *International Journal of Multiphase Flow*, Vol. 29, pp. 721-750, 2003-05.
- [27] JENNY, PATRICK AND ROEKAERTS, DIRK AND BEISHUIZEN, NIJSO, “Modeling of turbulent dilute spray combustion”, *Progress in Energy and Combustion Science*, Vol. 38, pp. 846-887, 2012-12.
- [28] ABOU AL-SOOD, M. M. AND BIROUK, M., “A numerical study of the effect of turbulence on mass transfer from a single fuel droplet evaporating in a hot convective flow”, *International Journal of Thermal Sciences*, Vol. 46, pp. 779-789, 2007-08.
- [29] DOWNING, C.G., “The evaporation of drops of pure liquids at elevated temperatures: rates of evaporation and wet-bulb temperatures”, *AIChE Journal*, Vol. 12, pp. 760-766, 1966.
- [30] CHIN, J.S., AND LEFEBVRE, A.H., “The Role of Heat-up Period in Fuel Drop Evaporation”, *Int. J. Turbo Jet Engines*, Vol. 2, pp. 315-325, 1985.

- [31] KOLAITIS, D.I., FOUNTI, M. A., “A comparative study of numerical models for Eulerian-Lagrangian simulations of turbulent evaporating sprays”, *International Journal of Heat and Fluid Flow*, Vol. 27, pp. 424-435, 2006.
- [32] MILLER, R.S., HARSTAD, K. AND BELLAN, J., “Evaluation of equilibrium and non-equilibrium evaporation models for many-droplet gas-liquid flow simulations”, *International Journal of Multiphase Flow*, Vol. 24, pp. 1025-1055, 1998.
- [33] MONGIA, H.C. AND MOSTAFA, A.A., “On the modeling of turbulent evaporating sprays: Eulerian versus Lagrangian approach”, *Int. J. Heat Mass Transfer*, Vol. 30, pp. 2583-2593, 1987.
- [34] ELGHOBASHI, S. E. AND MOSTAFA, A. A., “A two-equation turbulence model for jet flows laden with vaporizing droplets”, *Int. J. Multiphase flow*, Vol. 11, pp. 515-533, 1985.
- [35] ADHIRAJ KISHORE DASGUPTA., Numerical Simulation of Dilute Gas-Particle flows using Eulerian-Eulerian approach in a General Purpose CFD Solver, Thesis for the Degree of Master of Technology, *Department of Mechanical Engineering*, Indian Institute of Technology Kanpur, 2008.
- [36] BOKADE V.K., “CFD Analysis of a Low Pressure Chemical Vapor Deposition Reactor”, Thesis for the Degree of Master of Technology, *Department of Mechanical Engineering*, Indian Institute of Technology Kanpur, 2004.
- [37] CHEN, X.Q., AND PEREIRA, J.C.F., “Computation of turbulent evaporating sprays with well-specified measurements: a sensitivity study on droplet properties”, *Int. J. of Heat and Mass Transfer*, Vol. 39, pp. 441-454, 1996.
- [38] SHASHWAT SWAMI JAISWAL., Numerical Simulation of Dilute Gas-Droplet flows, Thesis for the Degree of Master of Technology, *Department of Mechanical Engineering*, Indian Institute of Technology Kanpur, 2008.

- [39] DAIF, A., BOUAZIZ, M., CHESNEAU, X. AND CHERIF, A.A., "Comparison of multicomponent fuel droplet vaporization experiments in forced convection with the Sirignano model", *Exp. Thermal Fluid Sci.*, Vol. 18, pp. 282-290, 1999.
- [40] ESWARAN V. ET AL., "Development of a General Purpose Robust CFD Solver", Project Report No. 1, *Department of Mechanical Engineering*, Indian Institute of Technology Kanpur, December, 2005.
- [41] FLUENT 6.2 DOCUMENTATION, *Fluent Inc. Lebanon, NH*
- [42] CHEN C.P., WOOD P.E., "A Turbulence Closure Model for Dilute Gas-Particle Flows" *The Canadian Journal Of Chemical Engineering*, Vol. 63, pp. 349-359, 1985.
- [43] HWANG, T.H., "Laminar droplet flow in combined hydrodynamically and thermally developed region of circular tubes", *Int. Comm. Heat Mass Transfer*, Vol. 17, pp. 703-710, 1990.
- [44] TU J.Y., "Computation of Turbulent Two Phase Flow on Overlapped Grids", *Numerical Heat Transfer, Part B: Fundamentals*, Vol. 32, pp. 175-195, 1997.
- [45] KOLEV, N.I., "Multiphase flow dynamics", *Springer-Verlag*, Vol. 2, 2005.
- [46] KORDULLA W. AND VINOKUR M., "Efficient Computation of Volume in Flow Predictions", *AIAA Journal*, Vol. 21, pp. 917-918, 1983.
- [47] KUO, K. K. Y., "Principles of Combustion", *John Wiley and Sons, New York*, 1986.
- [48] ALEXANDRE FAVRE, "Turbulent transport in compressible flows", *Institut de Mechanique Statistique de la Turbulence*, 1965.
- [49] NARASIMHA REDDY RAPAKA, "Implementation of Eddy Viscosity Turbulence Models in a General Purpose CFD Solver", Thesis for the Degree of Master of Technology, *Department of Mechanical Engineering*, Indian Institute of Technology Kanpur, 2006.

-
- [50] PATANKAR S.V., "Numerical Heat Transfer and Fluid Flow", *Taylor and Francis*, 2004.
- [51] PRAKASH S., ESWARAN V., BISWAS G., MURALIDHAR K. AND DHANDE S.G., "Numerical Simulation of Unsteady Three-Dimensional Flow Around an Elongated Body Moving in an Incompressible Fluid Using a Parallel Computer", Technical Report, *DRDL Report*, Hyderabad, July 1996.
- [52] RHIE C.M. AND CHOW W.L., "Numerical Study of the Turbulent Flow Past an Airfoil with Trailing Edge Separation", *AIAA Journal*, Vol. 21, No. 11, pp. 1525-1532, 1983.